https://doi.org/10.5194/egusphere-2023-1725
Preprint. Discussion started: 6 September 2023

Soil moisture-atmosphere coupling strength over Central Europe in the recent warming climate

Thomas Schwitalla[1], Lisa Jach[1], Volker Wulfmeyer[1], Kirsten Warrach-Sagi[1]

[1]Institute of Physics and Meteorology, University of Hohenheim, Garbenstrasse 30, 70599 Stuttgart, Germany

Correspondence to: Thomas Schwitalla (Thomas.Schwitalla@uni-hohenheim.de)

Abstract

In the last decades, Europe more often experiences periods of severe drought and heatwaves which have a major impact on agriculture and society. While land surface conditions were found to be crucial for exacerbating duration and intensity of these events, their influence is typically quantified for climate periods or single events. To provide an overview of how surface conditions shape land-atmosphere (LA) coupling, this study investigates interannual variability of LA coupling strength for the summer seasons 1991-2022 over Europe. The focus is set on the warm summers and the analysis is based on ERA5.

Especially the drought summer seasons 2003, 2018, and 2022 can be identified by the changing soil moisture-atmosphere coupling pattern in turn leading to an increased lifted condensation level height inhibiting local deep convection triggering. Summer 2021 was a special case as spring precipitation was on average and a heavy rain event occurred during July, resulting in high moisture availability leading to a change in the LA feedback strength. During the four warm and wet summers since 1991 no strong soil moisture-atmosphere coupling is observed as there is always enough soil moisture available for evaporation. The results obtained with respect to LA coupling strength reflect a shift in the coupling relationships toward reinforced heating and drying by the land surface under heatwave and drought conditions, whose frequency is increasing with ongoing climate change.

1 Introduction

In the last decades, Europe experienced severe drought periods and heatwaves (WMO, 2015; C3S, 2018; WMO, 2022a) where 2022 was the hottest summer ever recorded over Europe (WMO, 2022a). Precipitation exhibited a strong dry anomaly over Central Europe in 2003, 2018 and 2022 (WMO, 2004, 2018; C3S, 2018; WMO, 2022b; Spensberger et al., 2020). At the same time, the soil experienced an exceptional dryness in the uppermost 25 cm (Boeing et al., 2022; Rakovec et al., 2022) as shown by the soil moisture index developed by Zink et al. (2016). This was also shown by Rousi et al. (2023) and Dirmeyer et al. (2021) for 2018, who suggest that these extreme conditions will be more likely under climate change conditions where two out of three summer seasons will experience hot and dry conditions. Rousi et al. (2022) identified Europe as a heatwave hot spot where heat waves are three to four times more likely than in other areas of the midlatitudes due to the occurrence of double-jet stream situations (Kornhuber et al., 2017).

Land-atmosphere (LA) coupling generally describes the co-variability of atmospheric conditions (e.g., planetary boundary layer (PBL) height, convective available potential energy (CAPE), lifted condensation level (LCL)) and the condition of the land surface (e.g., vegetation, soil moisture) (Findell and Eltahir, 2003b; Koster et al., 2004; Dirmeyer, 2011; Guo et al., 2006). In the context of extremes, it was identified as a driver and intensifier for the duration and intensity of heat waves and droughts (van Heerwaarden and Teuling, 2014; Ukkola et al., 2018;

https://doi.org/10.5194/egusphere-2023-1725
Preprint. Discussion started: 6 September 2023

Schumacher et al., 2022). Miralles et al. (2019) and Schumacher et al. (2022) showed the existence of a self-propagating mechanism of droughts. Meteorological droughts intensify due to increased water vapor deficit (VPD) inside the PBL which feeds back into an intensified depletion of surface moisture reservoirs.

One of these reservoirs is soil moisture, which plays a key role for the climate due to its influence on the partitioning between surface sensible and latent heat fluxes of the incoming solar energy (Seneviratne et al., 2010; Stephens et al., 2023). In vegetated areas the surface latent heat flux additionally depends on the atmospheric water vapor deficit (VPD), air temperature, incoming radiation, and vegetation properties (stomatal resistance, leaf area index (LAI) and rooting depth) (Miralles et al., 2019; Warrach-Sagi et al., 2022). In consequence of spatial and temporal variability in these influencing factors, LA feedback often shows regional, but also temporal variations, especially under climate change conditions (Seneviratne et al., 2006; Denissen et al., 2022; Jach et al., 2022).

Knist et al. (2017) investigated the long-term average relationship between root zone soil moisture and surface fluxes by means of different regional climate model (RCM) simulations for the period 1989-2008 for the European summer seasons. They identified a coupling hot spot region for the surface coupling of sensible and latent heat fluxes and latent heat flux and 2-m temperature in South Europe while a transition zone is present over larger parts of Central Europe. Jach et al. (2022) performed a RCM LA coupling sensitivity experiment with respect to climate change signals of temperature and humidity for the period 1986-2015. Their results revealed a permanent coupling hot spot over Northeast and East Europe with the location being insensitive to changes in low level moisture and temperature. While there was only little sensitivity over the northern part of this area, Central Europe and the British Isles showed change in the coupling regime based on the CTP-HI_{low} framework (Findell and Eltahir, 2003a, 2003b). Warrach-Sagi et al. (2022) evaluated the atmospheric coupling index (ACI; Guo et al., 2006; Dirmeyer, 2011) and found a strong sensitivity between sensible heat flux and CAPE during the growing season 2005 over South Germany.

Several studies investigated the relation of soil moisture with recent European heat waves and droughts. Hauser et al. (2016) found that a soil moisture-temperature feedback was, among a wave train (Di Capua et al., 2021), a key driver for the severe heat wave over Siberia in 2010, while Dirmeyer et al. (2021) and Orth (2021) found that it was a key driver for the European heatwave in 2018. García-Herrera et al. (2010) found that a strong soil moisture deficit was also one of the key drivers for the 2003 European heat wave. The study of Miralles et al. (2014) suggest that the heatwaves over Europe in 2003 and over Russia in 2010 were enhanced by a persistent large scale weather pattern associated with a strong soil moisture decay. The analysis of Dirmeyer et al. (2021) for the 2018 European heatwave revealed enhanced soil moisture – near-surface feedback under drought conditions. The exceptionally low soil moisture limited evapotranspiration and thus amplified the heat wave due to reduced evaporative cooling (Santanello et al., 2018).This led to one of the most severe heatwaves over Europe since 1979 (Becker et al., 2022).

Wehrli et al. (2019) found that soil moisture and the large scale weather pattern are equally important for the duration and intensity of heatwaves around the globe. According to Ossó et al. (2022), Europe already faced an increase in climate extremes since 2000 and will remain a hot spot for severe droughts (Huebener et al., 2017; van der Wiel et al., 2022) impacting not only summer's crop yields (Toreti et al., 2022) but also affecting the generation of renewable energy.

The in the preceding paragraph described shifts in the hydrological conditions from energy- to moisture-limited conditions originating from droughts and heatwaves (Dirmeyer et al., 2021; Duan et al., 2020) or severe flooding (Lo et al., 2021) imply temporal variability in LA coupling at sub-seasonal to interannual time-scales. Guo and Dirmeyer (2013) also found interannual variability in soil moisture-precipitation coupling in consequence of

https://doi.org/10.5194/egusphere-2023-1725
Preprint. Discussion started: 6 September 2023

different soil moisture availability. Additionally, the critical soil moisture thresholds (Dirmeyer et al., 2021; Rousi et al., 2023) suggest not only an intensification of the heat and drought conditions by LA coupling over Europe but also a strengthening of the coupling itself. However, a quantification of temporal variability in different coupling relationships, as well as understanding of the impact of the variability remain lacking, as LA coupling strength was barely investigated over Europe, and particularly on other time scales than climate periods, so far. The same applies to shifts between coupling regimes due to variability in the climatic conditions.

In this study, we therefore assess the temporal variability of LA coupling of the European summer seasons 1991-2022 on the interannual time scale in dependence on temperature, soil moisture, precipitation and large-scale weather pattern by applying data from the fifth generation European Centre for Medium Range Weather Forecasting (ECMWF) atmospheric reanalysis (ERA5; Hersbach et al., 2020) and the ENSEMBLES daily gridded observational dataset for precipitation (E-OBS; Cornes et al., 2018).

The paper is structured as follows: Section 2 describes the applied data sets, selected coupling indices and the classification of the 32 summer seasons 1991-2022. Section 3 describes the large-scale weather pattern with respect to 500 hPa geopotential, 2-m temperatures, precipitation, and soil moisture followed by the LA coupling analysis in section 4. Section 5 summarizes our results providing an outlook for potential future research.

2 Material and Methods

2.1 Datasets

For the analysis of the LA feedback regions, the fifth generation European Centre for Medium Range Weather Forecasting (ECMWF) atmospheric reanalysis (ERA5; Hersbach et al., 2020) was used. ERA5 is produced by the Copernicus Climate Change Service (C3S, http://climate.copernicus.eu/) at ECMWF. This data set provides hourly estimates of atmospheric, surface, and oceanic variables on a horizontal resolution of ~ 30 km and includes the assimilation of observations. Following the World Meteorological Organization's (WMO) recommendation to adjust the climate normal period (WMO, 2017), the summer seasons of 1991-2020 serve as reference period for the calculation of anomalies. The investigation period covers the summer seasons between 1991-2022 over an area between 11°W-30°E and 35°N-70°N (see Fig. 1). Reasons to choose very recent summers were, among others, that the first half of summer 2021 was very warm and dry while an extreme precipitation event (Mohr et al., 2023) led to a sudden increase in soil moisture over France, Benelux, and West Germany. Summer 2022 was the hottest summer seasons ever recorded over Europe associated with a west-east soil moisture anomaly pattern (C3S, 2022). Overall, both recent summer seasons reflect the climate change trend over Europe.

To categorize the summer seasons during this period into warm and wet, warm and dry, and cold summer seasons, seasonal mean anomalies of ERA5 2-m temperatures and the ENSEMBLES daily gridded observational dataset for precipitation (E-OBS; Cornes et al., 2018) version V26.0e precipitation were calculated. To complement our analysis, seasonal mean anomalies of 500 hPa geopotential (Lhotka and Kyselý, 2022) and ERA5 volumetric root zone soil moisture were calculated.

All anomalies were calculated using the Climate Data Operators (CDO) version 2.0.5 (Schulzweida, 2022).

2.2 LA coupling indices

In our study we apply the statistical LA feedback metrics, namely the terrestrial coupling index (TCI) and atmospheric coupling index (ACI), described in Guo et al. (2006), Dirmeyer (2011), and Santanello et al. (2018).

https://doi.org/10.5194/egusphere-2023-1725
Preprint. Discussion started: 6 September 2023

To calculate the different indices, we used a combination of the NCAR Command Language (NCL, Brown et al., 2012) together with the FORTRAN programs provided by Tawfik (2015).

For our analysis, we used volumetric root zone soil moisture η, defined as weighted sum of the soil moisture in the top three soil layers of ERA5 down to 1 m below the surface, surface latent and sensible heat fluxes (LH and SH), CAPE, and PBL height (PBLH). In addition, we used the lifted condensation height (HLCL) and the lifted condensation height deficit (LCL deficit), defined as difference between HLCL and PBLH. As HLCL was not available from ERA5, we used the approach from Georgakakos and Bras (1984) and Bolton (1980) which is based on surface pressure, 2-m temperature, and 2-m dewpoint to derive HLCL which is also applied in Dirmeyer et al. (2014).

The strength of the TCI (Eq. 1) is defined as

$$TCI = \sigma(\eta)\frac{dLH}{d\eta} \quad (1)$$

where $dLH/d\eta$ is the slope of the linear regression between the surface latent heat flux (LH) and the root zone soil moisture η as described in Santanello et al. (2018). It describes the sensitivity of LH with respect to changes in the root zone soil moisture. To derive the strength of the coupling between the land surface and the atmosphere (ACI), soil moisture can, e.g., be substituted by surface fluxes in Eq. 1 while LH can be substituted by the planetary boundary layer height, or CAPE (Dirmeyer et al., 2014).

The daily mean values are calculated between 06 UTC and 18 UTC (Yin et al., 2023) as e.g., the surface latent heat fluxes during night-time becomes close to zero with very little variations during this time. Also, during night-time, PBLH collapses to small values and stays often constant which has a detrimental impact on the LA-feedback analysis. Water grid cells are not considered in our evaluation.

2.3 Classification of summer seasons

For the classification of the summer seasons with respect to temperature and precipitation (Table 1), we calculated the spatial median of the 2-m temperature from ERA5 and precipitation anomalies from E-OBS with respect to the summer mean 1991-2020 over Europe. If the temperature anomaly median is positive, the summer season is classified as warm, if the median of the precipitation anomaly is positive, the summer is classified as wet summer. For the classification only land grid cells between 36°N-70°N and 11°W-30°E were considered.

Year	1991	1992	1993	1994	1995	1996	1997	1998	1999	2000	2001	2002	2003	2004	2005	2006
T2	C	C	C	W	C	C	C	C	C	C	C	W	W	C	C	W
P	Dry	Wet	Wet	Dry	Dry	Dry	Wet	Wet	Dry	Dry	Wet	Wet	Dry	Wet	Wet	Dry
Year	2007	2008	2009	2010	2011	2012	2013	2014	2015	2016	2017	2018	2019	2020	2021	2022
T2	W	C	C	W	C	C	W	C	W	W	W	W	W	W	W	W
P	Wet	Wet	Wet	Wet	Wet	Dry	Dry	Wet	Dry	Dry	Wet	Dry	Dry	Dry	Dry	Dry

Table 1. Classification of the summer seasons 1991-2022 according to the median of 2-m temperature (T2) and precipitation (P) anomalies with respect to the 1991-2020 mean. C (cold) and W (warm) denotes temperatures below and above the climatological average 1991-2020.

The warm and dry summer seasons became the prevailing situation since 2013 as shown in Table 1. A strong reduction in annual and seasonal precipitation, combined with a reduced atmospheric water availability led to a

https://doi.org/10.5194/egusphere-2023-1725
Preprint. Discussion started: 6 September 2023

constant decline of the root zone soil moisture and thus an agricultural drought which was the case, e.g., in 2018-2020 over Europe (van der Wiel et al., 2022). The warm and wet summer seasons (2002, 2007, 2010, 2017) were additionally selected to investigate potential differences in the LA feedback as compared to the warm and dry summer seasons.

3 Results

The following subsections describe the characteristics of the warm and dry and warm and wet summer seasons chosen for evaluation (Table 1) with respect to 500 hPa geopotential, 2-m temperature, root zone soil moisture η, and precipitation anomalies.

3.1 Warm and dry summer seasons

Figure 1 shows the 500 hPa geopotential height anomalies for the summer seasons classified as warm and dry. The 500 hPa geopotential height helps to determine mid-tropospheric troughs and ridges describing the large-scale weather pattern. The warm and dry summer seasons are in general characterized by strong positive 500 hPa geopotential anomalies over major parts of Europe. However, summer 2015 and 2020 are exceptions. In 2015, a pronounced north-south anomaly gradient is visible with negative values over the British Isles and Scandinavia while in 2020 the 500 hPa geopotential is only slightly above the average 1991-2020 (bottom right panel in Fig. 1).

The positive geopotential anomalies are associated with positive 2-m temperature anomalies with the highest anomalies present in 2003, 2018, 2019, and 2022 (Fig. 2). Precipitation (Fig. 3) is often below the climatological average 1991-2020 while a precipitation surplus exists over the Balkan region. Root zone soil moisture (Fig. 4) is mainly on the dry side with 2022 being the driest season of the investigation period (bottom right panel in Fig. 4). The positive soil moisture anomaly during summer 2013 is related to a major precipitation surplus in spring as compared to the climatological average. This was mainly caused the severe flooding event at the end of May 2013 over Germany and its neighboring countries (Grams et al., 2014) and convective precipitation events in France in the second half of June 2013. The well above soil moisture during summer 2016 is related to the heavy rain over France and Germany at the end of May 2016 until the beginning of June 2016 (Piper et al., 2016).

Although temperatures in 2021 were above the climatological average 1991-2020, precipitation over France, Benelux, and Germany was above average due to a small scale low-pressure system which caused the Ahr flood event (Mohr et al., 2023) (bottom row in Fig 3). Although our target region is Germany and its neighboring countries, summer 2021 is still considered as warm and dry in our study as the precipitation anomaly remains negative over East and Southeast Europe, Scandinavia, and the Iberian Peninsula.

It is worth to note is that out of the 32 summer seasons investigated in this study, 8 warm and dry summer seasons belong to the period 2010-2022.

https://doi.org/10.5194/egusphere-2023-1725
Preprint. Discussion started: 6 September 2023

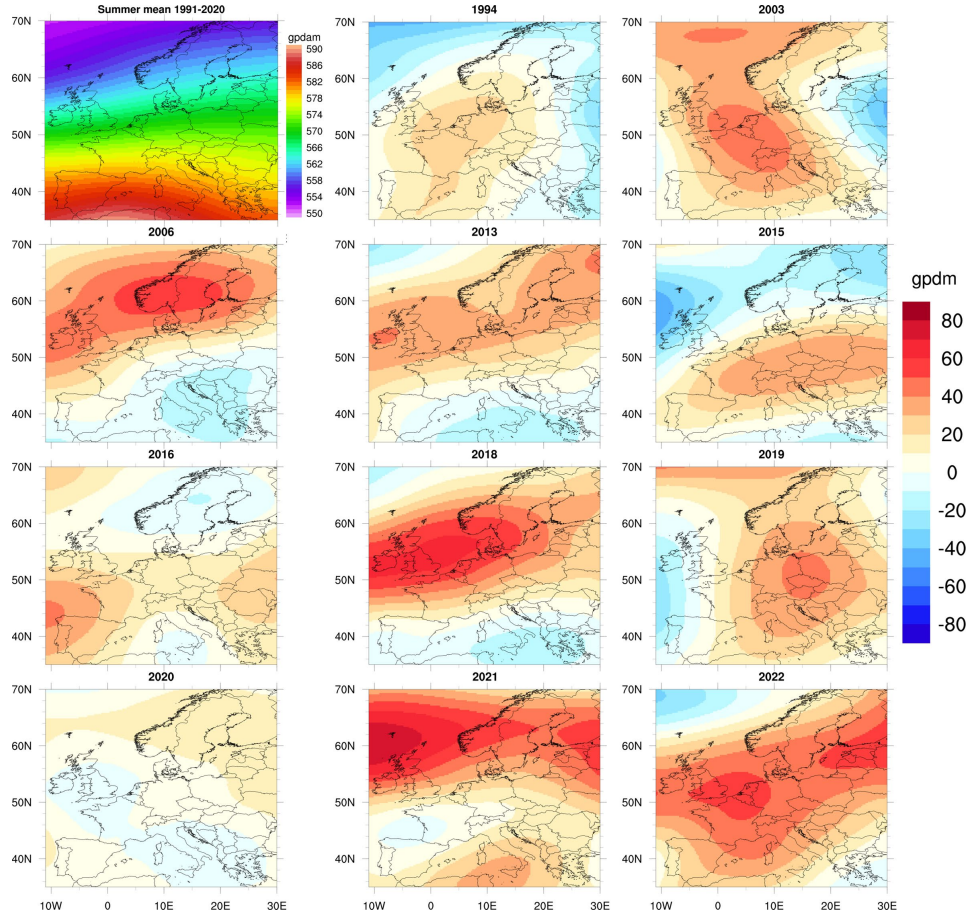

Figure 1. ERA5 500 hPa geopotential anomalies with respect to 1991-2020 of the dry and warm summer seasons. The top left panel denotes the mean summer geopotential height 1991-2020.

180

https://doi.org/10.5194/egusphere-2023-1725
Preprint. Discussion started: 6 September 2023

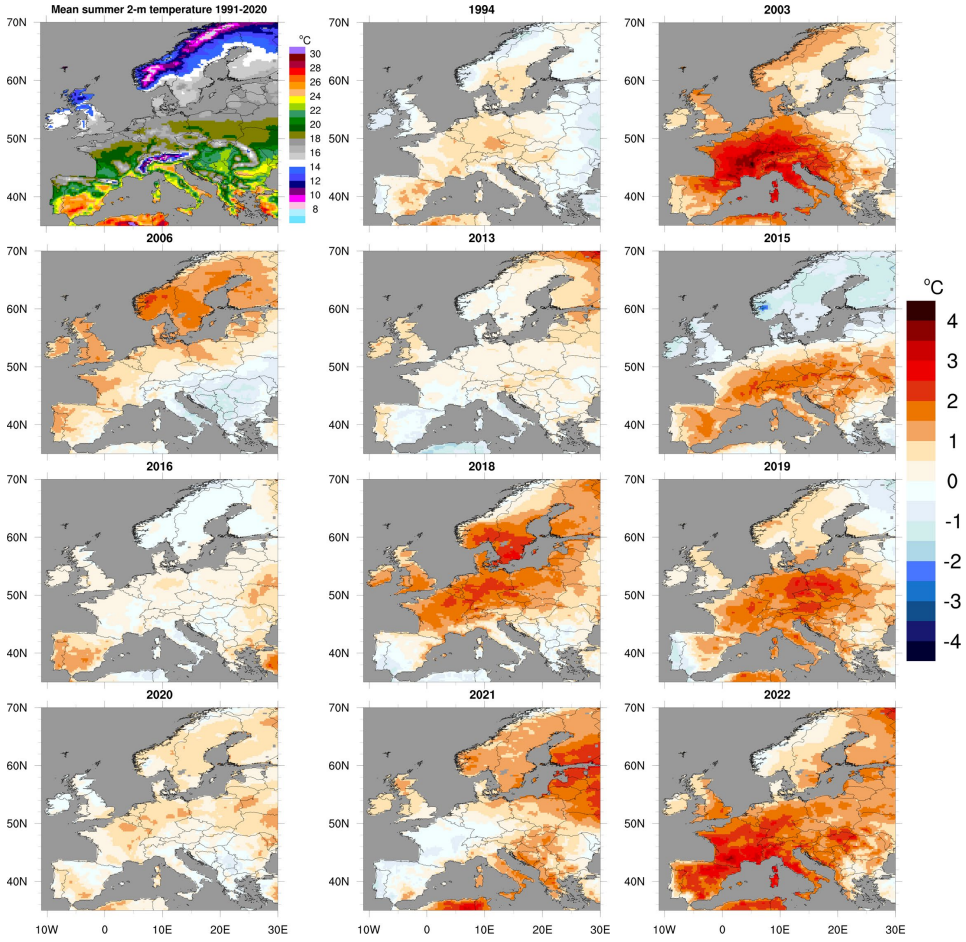

Figure 2. ERA5 2-m temperature anomalies for the warm and dry summer seasons. The top left panel shows the mean summer 2-m temperatures 1991-2020 from ERA5.

https://doi.org/10.5194/egusphere-2023-1725
Preprint. Discussion started: 6 September 2023

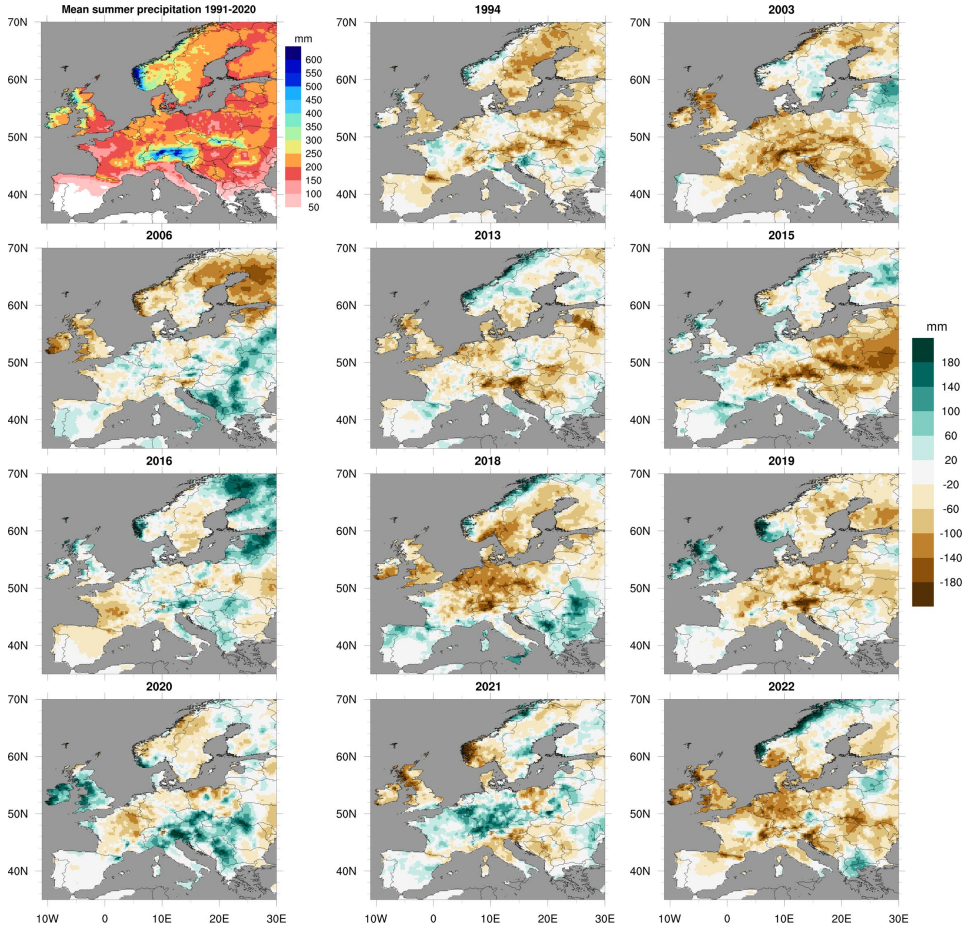

Figure 3. E-OBS precipitation anomalies for the warm and dry summer seasons. The top left panel denotes the mean summer precipitation 1991-2020.

https://doi.org/10.5194/egusphere-2023-1725
Preprint. Discussion started: 6 September 2023

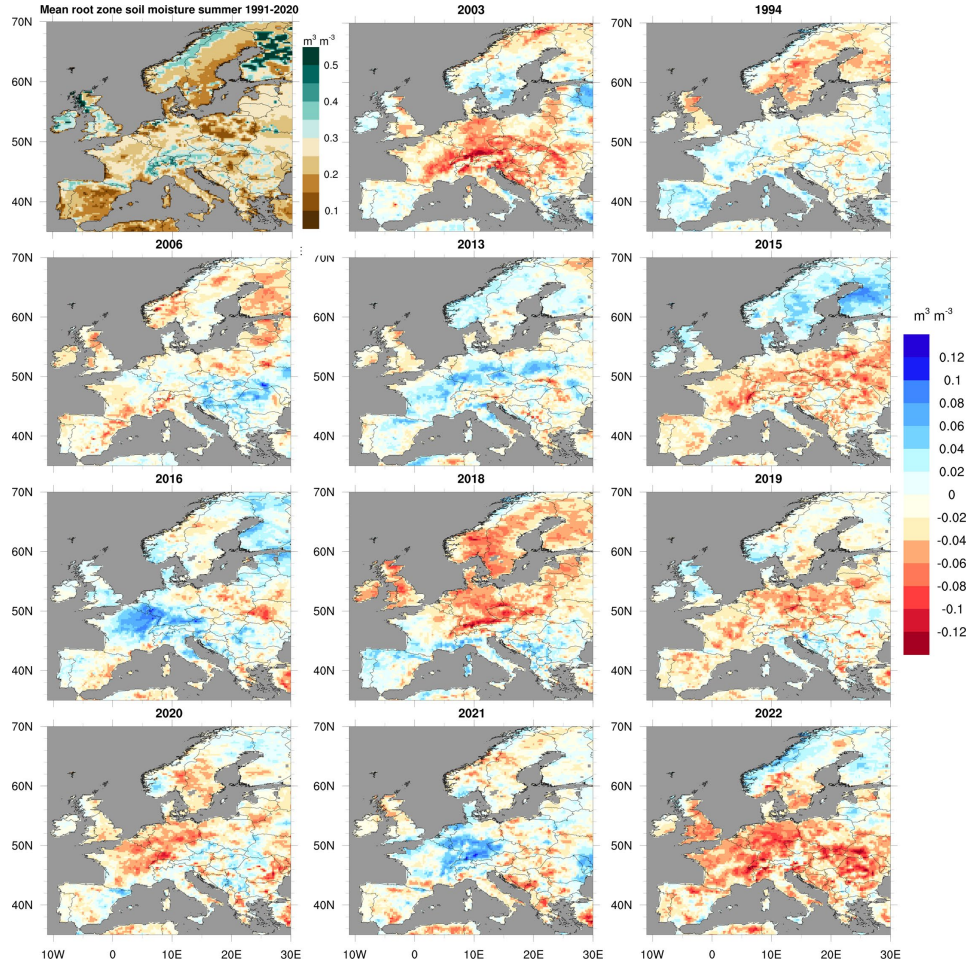

Figure 4. ERA5 soil moisture anomalies with respect to 1991-2020 for the summer seasons categorized as warm and dry. The top left panel denotes the summer mean root zone soil moisture 1991-2020 from ERA5

3.2 Warm and wet summer seasons

185 Figure 5 shows the 500 hPa geopotential anomalies for the four warm and wet summer seasons 2002, 2007, 2010, and 2017.

https://doi.org/10.5194/egusphere-2023-1725
Preprint. Discussion started: 6 September 2023

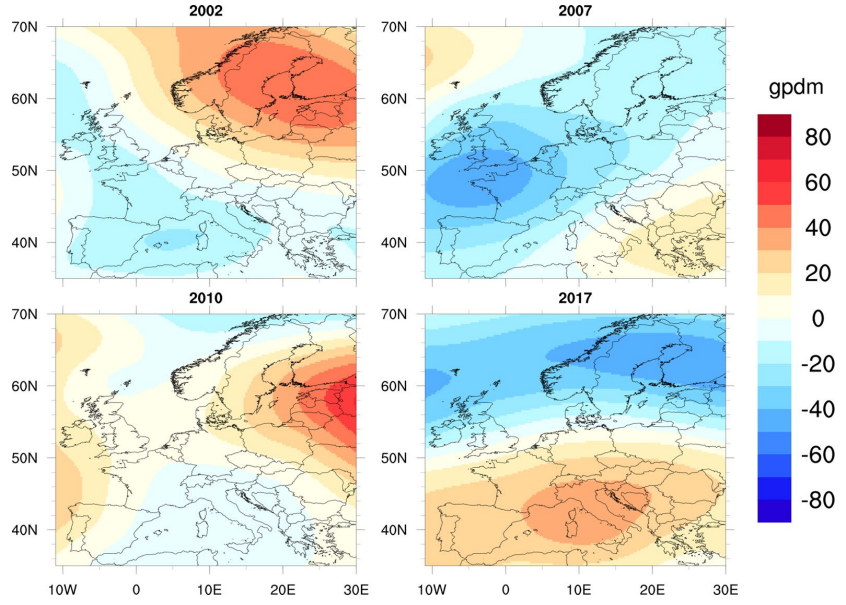

Figure 5. Same as Fig. 1 but for the warm and wet summer seasons 2002, 2007, 2010, and 2017. The climatological mean 1991-2020 is shown in the upper left panel of Fig. 1.

Compared to the seasons described in the precious section, 2002 shows a SW-NE geopotential anomaly gradient with high anomalies over Scandinavia while 2007 shows negative geopotential height anomalies over large areas of Europe. 2010 shows only weak geopotential anomalies over major parts of West and Central Europe, while strong positive anomalies are observed over East Europe related to the Russian heat wave (Becker et al., 2022). In 2017, the gradient shows a strong south-north gradient with zero values along 52°N north. 2007 shows a Quadrupole structure with positive anomalies over West and East Europe and weak negative anomalies over the Mediterranean. It is worth to note here that three of the seasons belong to the zonal circulation pattern where the main flow is clearly west-east oriented (Werner and Gerstengarbe, 2010).

The temperature anomalies (Fig. 6) clearly reflect the geopotential anomalies shown in Fig. 5 with a positive anomaly in 2002 over NE Europe and 2017 south of 52°N. During 2007, West Europe shows a clear negative anomaly while the Balkan region shows a moderate positive anomaly while 2010 shows distinct positive anomaly over East Europe as an extension of the Russian heat wave. By comparing Fig. 6 and 7, it is seen that positive temperature anomalies do not necessarily lead to a negative precipitation anomaly as during the summer (see later in section 4.3.2). This points toward more localized precipitation events related to an enhanced atmospheric instability (see later in section 3.3).

The root zone soil moisture mostly shows a neutral to wet anomaly (Fig. 8) while in 2017 the regions south of 52°N showed a root zone soil moisture dry bias (lower right panel in Fig. 8). The dry anomaly is related to an exceptionally dry spring season 2017 (C3S, 2017).

https://doi.org/10.5194/egusphere-2023-1725
Preprint. Discussion started: 6 September 2023

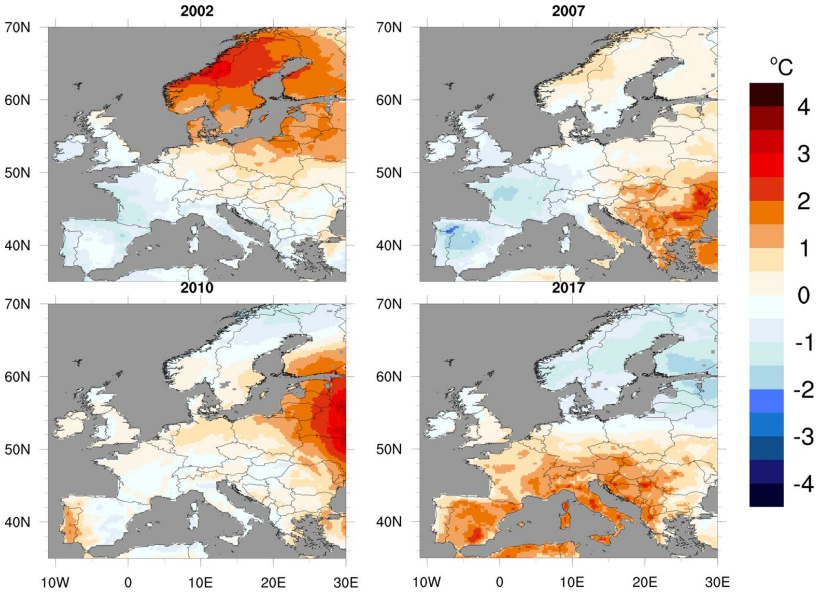

Figure 6. Same as Fig. 2 but for the warm and wet summer seasons 2002, 2007, 2010, and 2017. The climatological mean 1991-2020 is shown in the upper left panel of Fig. 2.

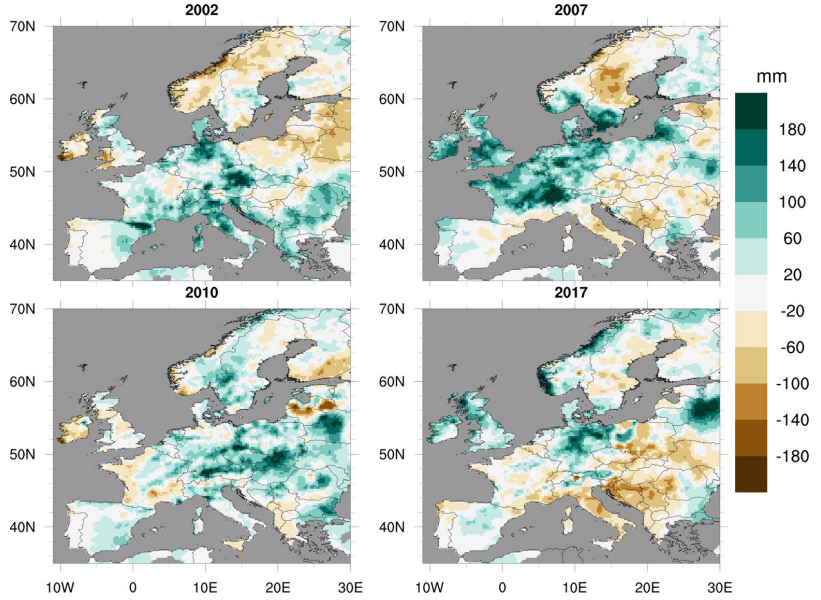

Figure 7. Same as Fig. 3 but for the warm and wet summer seasons 2002, 2007, 2010, and 2017. The climatological mean 1991-2020 is shown in the upper left panel of Fig. 3.

https://doi.org/10.5194/egusphere-2023-1725
Preprint. Discussion started: 6 September 2023

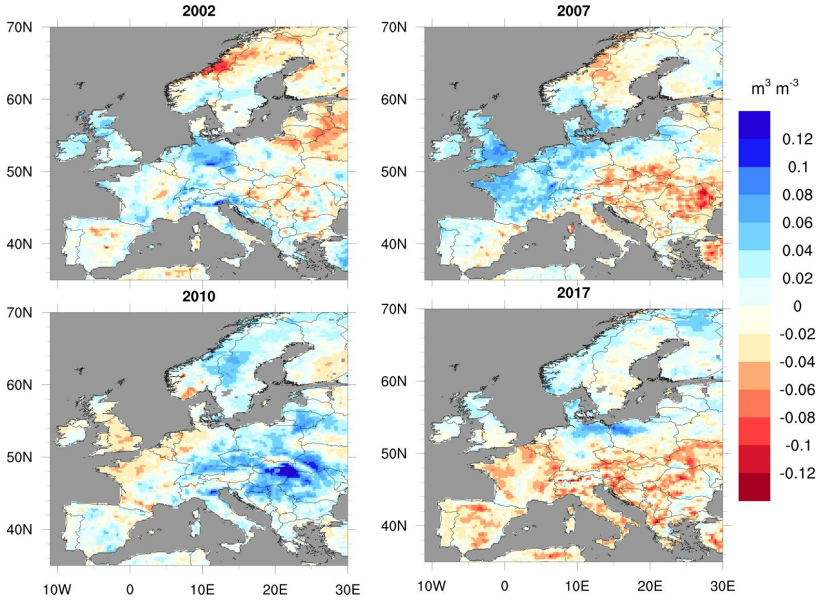

Figure 8. Same as Fig. 4 but for the summer seasons categorized as warm and wet (see Table 1). The climatological mean 1991-2020 is shown in the upper left panel of Fig .4.

4 Results

4.1 Terrestrial coupling strength

In this section, we will present the terrestrial coupling index following Dirmeyer (2011) for the selected summer seasons . As we are interested in daytime properties, we only used data between 06 UTC and 18 UTC to derive daily mean values from ERA5. According to Findell et al. (2015), a 92 day period is sufficient for LA feedback analysis on individual data sets.

In addition, the Pearson correlation coefficient between surface sensible (SH) and latent heat flux (LH) is shown which can also be used as an indicator for LA coupling (Knist et al., 2017). Water grid cells are not considered for the analysis.

4.1.1 Warm and dry summer seasons

Fig. 9 shows the TCIs of the summer seasons categorized as warm and dry which became the dominant situation over Europe since 2013. The TCI between η and LH describes how changes in soil moisture drives variations in the surface latent heat flux. A positive TCI denotes that LH is limited by the root zone soil moisture and the soil moisture variation results in LH variation while a negative TCI indicates that the development of LH is energy limited, i.e., the incoming energy determines the LH development. In case the absolute TCI is low, either there is too little soil moisture available for evaporation, close to the wilting point, or the soil is too wet and a further increase does not lead to considerable changes in evaporation (Müller et al., 2021). The very warm and dry seasons 2003, 2018, and 2022 show a strong positive TCI over the regions affected by low soil moisture (Fig. 4) while during the other seasons, the TCI over most parts of Europe is still positive, although with lower values of -20 W

https://doi.org/10.5194/egusphere-2023-1725
Preprint. Discussion started: 6 September 2023

m^{-2} as, e.g., shown in the CROP experiment described in Warrach-Sagi et al. (2022). During 2021, when a positive η anomaly is observed over Germany and eastern France (C3S, 2021a, 2021b), the TCI becomes negative with values of about -20 W m^{-2}. The correlation LH-SH (Fig. 10) became negative south of 44°N maintaining positive values north of 46°N. During the most hot and dry summer 2003, 2018, and 2022, the correlation LH-SH became negative over Central Europe which is related to the anomalously warm and dry conditions during these summer seasons preventing a moisture limitation in the soil. In contrast, during the warm and dry summer seasons 2013 and 2016 the correlation LH-SH stays positive. This could be related to the fact that in both years the spring seasons had a strong positive water balance because of heavy precipitation during this time (Grams et al., 2014; Piper et al., 2016).

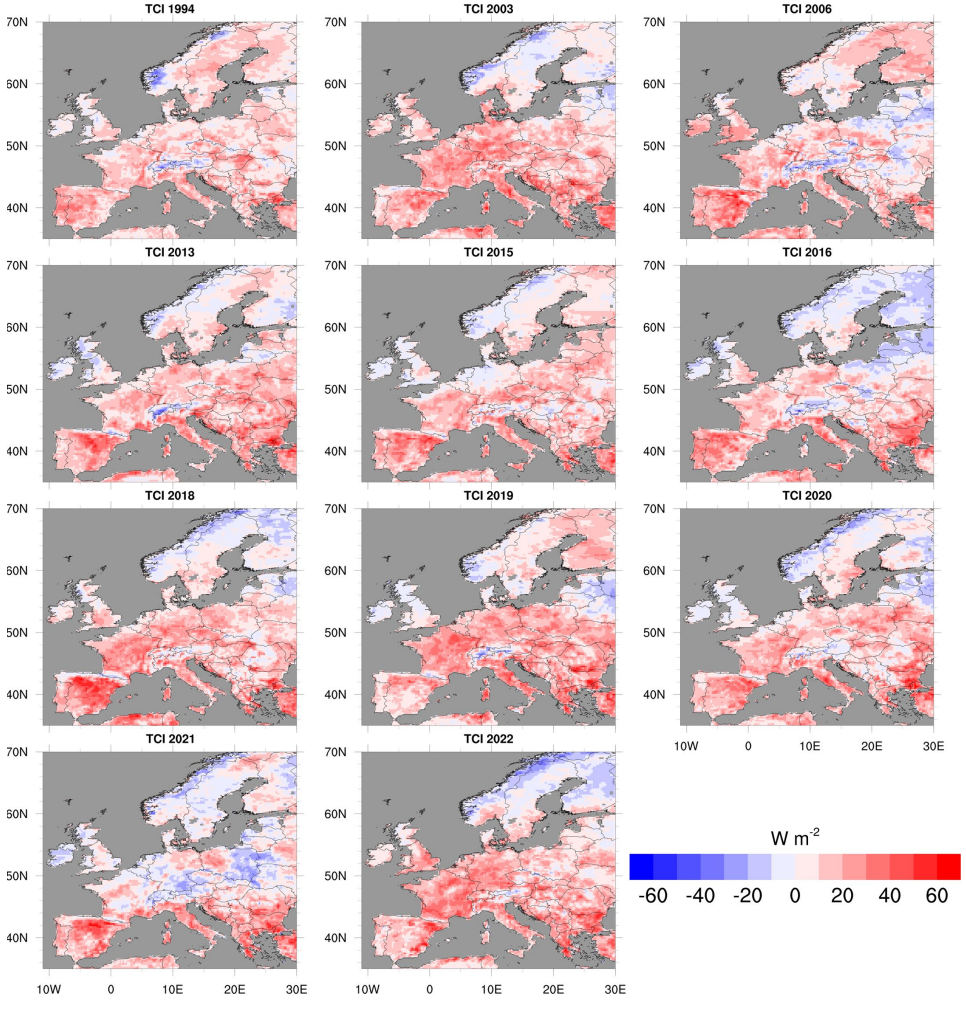

Figure 9. ERA5 based Terrestrial coupling indices (TCI) between root zone soil moisture η and surface latent heat flux (LH) for the warm and dry summer seasons presented in Fig. 1.

https://doi.org/10.5194/egusphere-2023-1725
Preprint. Discussion started: 6 September 2023

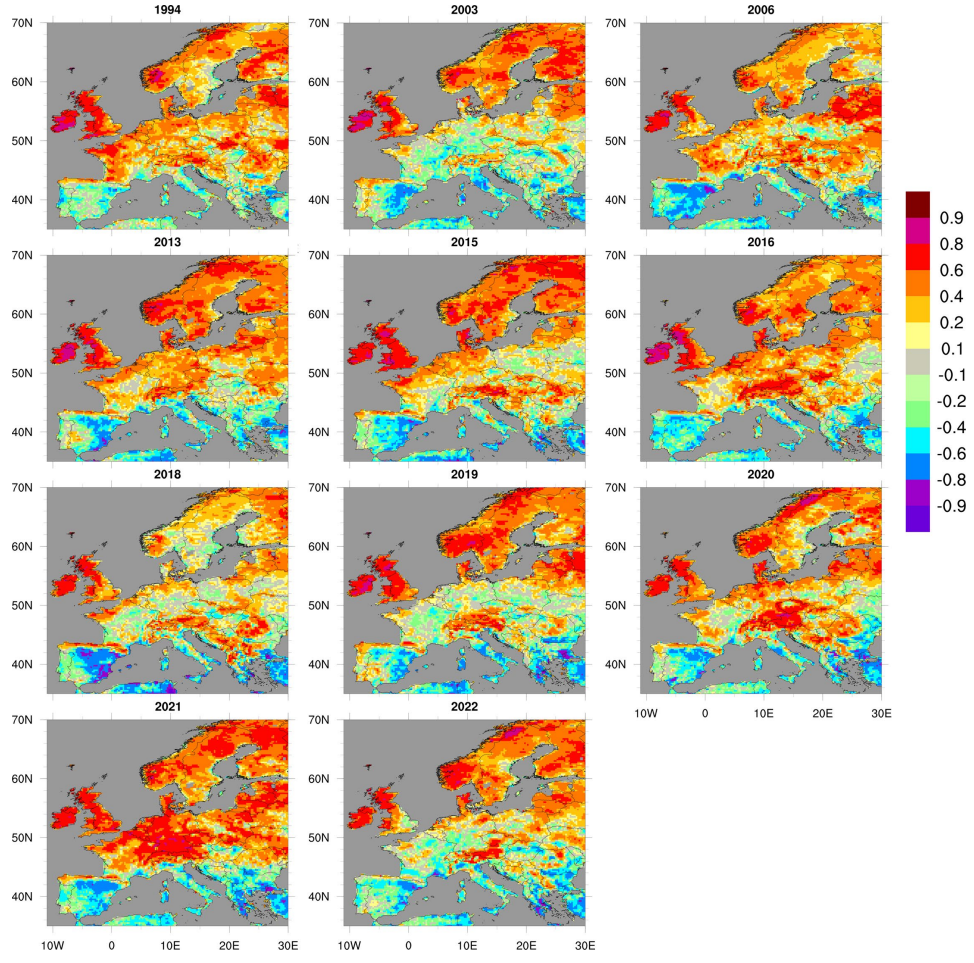

Figure 10. Pearson correlation coefficient between SH and LH for the warm and dry summer seasons presented in Fig. 1. Dark grey areas denote water grid cells.

4.1.2 Warm and wet summer seasons

Figure 11 shows the TCI for the warm and wet summer seasons 2002, 2007, 2010, and 2017. 2007 shows a small to moderate positive η anomaly over Germany, southern Scandinavia, France, and the British Isles (Fig. 8) leading to negative TCI values over Germany while the TCI η-LH shows almost weak coupling over Germany and France. The positive TCIs over Scandinavia in 2002 are related to the strong positive temperature anomaly and positive 500 hPa geopotential anomalies (Fig. 5). During summer 2017 the TCI over Germany and Scandinavia is slightly negative, most probably related to the average soil moisture availability. Over the Iberian Peninsula and Southeast Europe, the TCI is always positive. The correlation SH-LH (bottom panel of Fig. 11) over Germany stays positive indicating sufficient soil moisture for the latent heat/sensible heat partitioning. Over the Iberian Peninsula and Southeast Europe, the correlation often reaches values close to -1 indicating a decoupling between SH and LH due to low soil moisture availability although certain regions in Spain and Portugal show non-significant values.

https://doi.org/10.5194/egusphere-2023-1725
Preprint. Discussion started: 6 September 2023

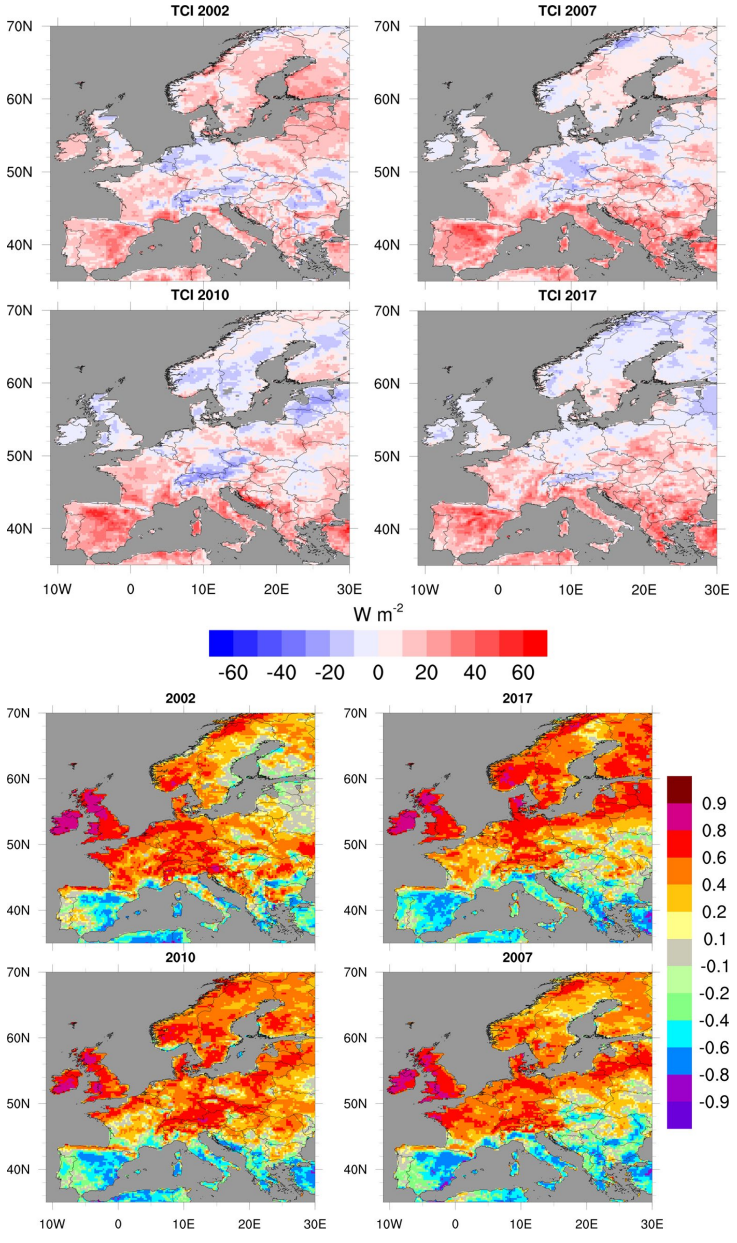

Figure 11. ACI (1st and 2nd row) and Pearson correlation coefficient (3rd and 4th row) between SH and LH for the warm and wet summers 2002, 2007, 2010, and 2017. Dark grey areas denote water grid cells.

4.2 Atmospheric Coupling strength

This section presents ACIs of the different summer seasons 1991-2022. ACIs are computed between LH and convective available potential energy (CAPE), LH and height of the lifted condensation level (HLCL).

https://doi.org/10.5194/egusphere-2023-1725
Preprint. Discussion started: 6 September 2023

To complement the analysis, the LCL deficit is shown in addition. The LCL deficit can be seen as a proxy for the evolution of the convective atmosphere as a positive LCL deficit inhibits convection developments (Santanello et al., 2009). CAPE depends on the atmospheric humidity which is, among others, related to LH while LH is related to the atmospheric temperature, humidity, soil moisture and LAI. Thus, an increase in LH leads to an increase of CAPE which indicates the potential for convective developments and thus precipitation.

Positive ACI values denote a dependence of the diurnal evolution of CAPE on the LH evolution while negative values show that CAPE is independent of the LH evolution but dependent on the atmospheric stratification. The lifted condensation level is the level above which saturation occurs and it sinks with increasing atmospheric humidity. Hence, negative ACI values denote a physical relationship between LH and HLCL, whereas a positive index signifies no coupling.

4.2.1 Warm and dry summer seasons

Figure 12 shows the ACI between LH and CAPE using daytime data between 06 UTC and 18 UTC for the warm and dry summer seasons.

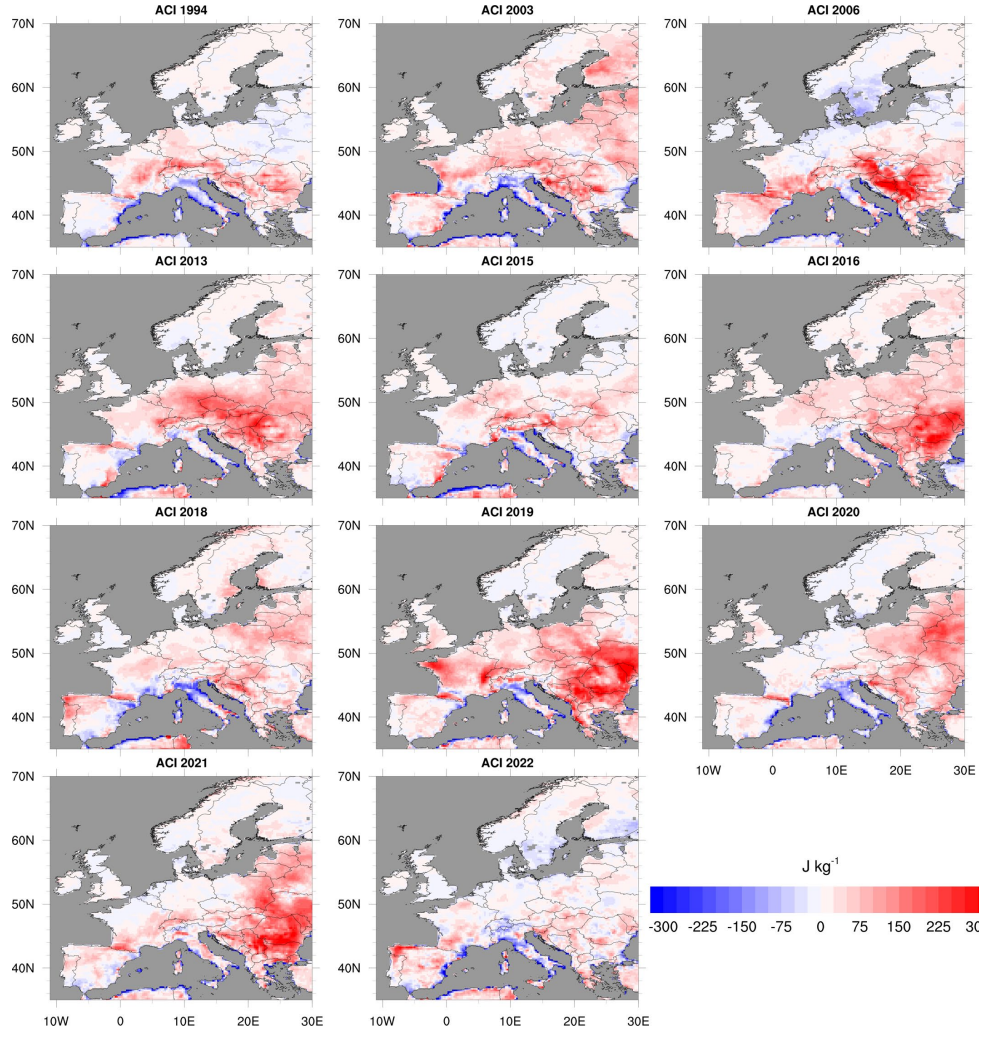

https://doi.org/10.5194/egusphere-2023-1725
Preprint. Discussion started: 6 September 2023

Figure 12. ERA5 based ACI between LH and CAPE for the warm and dry summer seasons. Grey areas denote water grid points.

A common feature is the negative ACI along the coast of the Mediterranean. As the sea surface temperatures in this region can reach up to 26°C (García-Monteiro et al., 2022), this leads to high evaporation over the sea and thus high precipitable water values (not shown). Together with a temperature gradient of up to 30 K or more in the Mediterranean between 850 hPa and 500 hPa (not shown), this leads to stronger atmospheric instability and thus reduced coupling to LH.

Coupling hot spots are observed over East Europe with ACI values of more than 250 J kg^{-1} occurring in connection with neutral or positive soil moisture anomalies in 2006, 2016, 2019, and 2021 (Fig. 4) which is connected to higher values of LH over these regions. Over Central Europe, only weak coupling is seen except for 2013 where major parts of central Europe exhibit a positive soil moisture anomaly.

The LCL deficit (Fig. 13), which can be interpreted as a proxy for the development of convection, is typically negative over northern Europe indicating that saturation and condensation mostly occurs within the PBL potentially leading to the formations of clouds and precipitation. Over southern Europe, the LCL deficit is usually positive inhibiting the formation of clouds. Over Central Europe the LCL deficit is comparatively small, unlike the years 2003, 2018, 2019, and 2022 which show strong positive values. These are the summers with a pronounced negative soil moisture anomaly and a strong positive temperature anomaly. Hence, the HLCL is higher than the planetary boundary layer height potentially leading to clear sky conditions and thus inhibiting convection (Santanello et al., 2011). As the TCI is mostly positive over Central Europe during these summers, while the ACI is neutral to slightly positive, this indicates that soil moisture variation impacts LH variations but with weak feedback to the atmosphere as indicated by the TLCI (Dirmeyer et al., 2014, Fig. S6).

Over the Iberian Peninsula, the LCL deficit is usually above 500 m and associated with a negative precipitation anomaly during summertime (see also Fig. 3) while the LCL deficit over the British Isles, Scandinavia, and West Russia stays negative throughout all warm and dry summer seasons. As at the same time the ACI between LH and CAPE shows also only small values, this suggest that the British Isles are more frequently impacted by large scale synoptic systems with a more stable atmosphere rather than localized precipitation events (Jach et al., 2020). The ACI between LH and HLCL usually shows positive values (except over the Iberian Peninsula, not shown) indicating that LH variations are not causally connected with variations of the HLCL.

Over Central Europe, the behavior for the most dry and warm summer seasons 2003, 2018, and 2022 however is different as Central Europe is in more often in the transition zone (Knist et al., 2017; Jach et al., 2022) and the LCL deficit became clearly positive (Fig. 14) inhibiting the probability for deep convection. At the same time, the ACI LH-HLCL shows neutral to slightly negative values indicating that the very dry soil during these summers (Fig. 3) caused the low LH which in turn initiated a considerable increase the HLCL. At the same time, the high SH (Fig. 10) leads to an increase of the PBL height and thus a higher LCL deficit as shown in Fig. 13 during the most hot and dry summer seasons. During summer 2021, Central Europe shows a positive soil moisture anomaly (Fig. 4) connected to weak or negative coupling between η and LH (Fig. 9). This means that LH shows little variations and thus lowering HLCL (Wei et al., 2021) which is also reflected neutral LCL deficit (bottom left panel in Fig. 13).

https://doi.org/10.5194/egusphere-2023-1725
Preprint. Discussion started: 6 September 2023

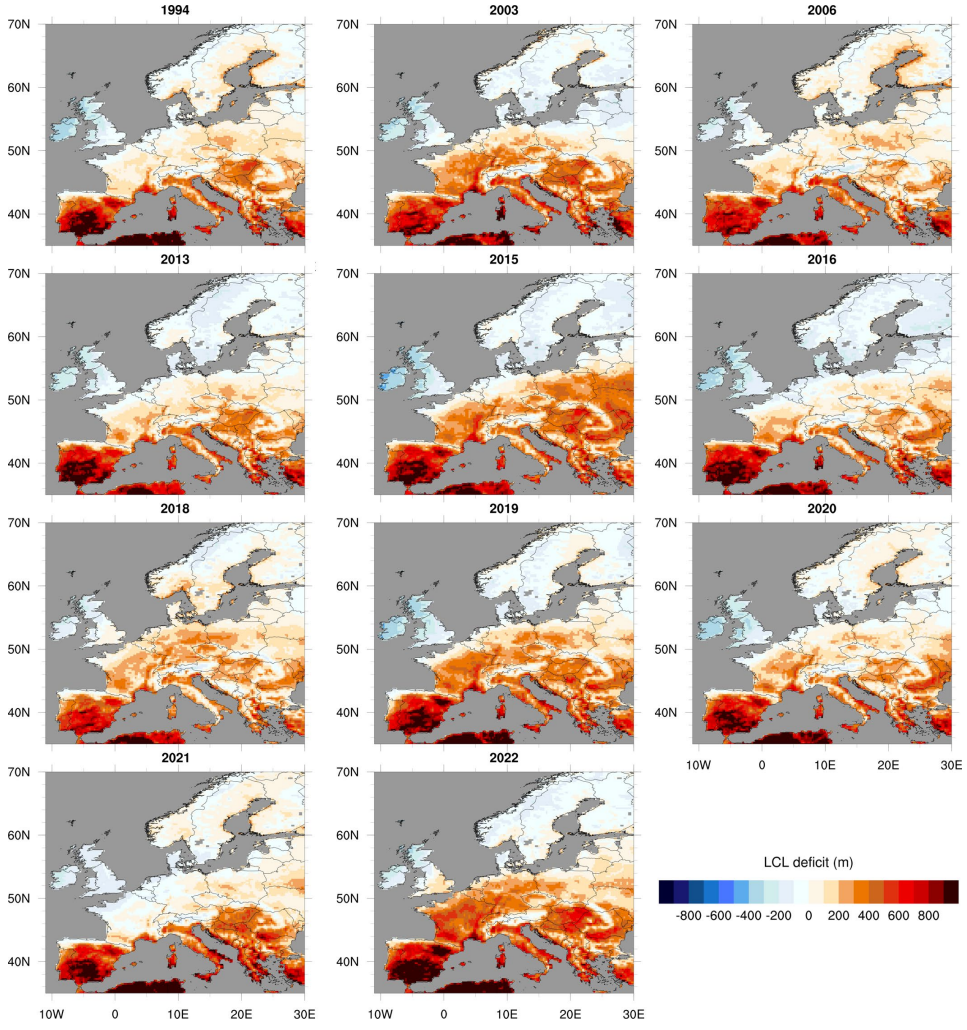

Figure 13. Mean ERA5 LCL deficit for the warm and dry summer seasons. Orange and reddish colors denote less favorable conditions for convection.

https://doi.org/10.5194/egusphere-2023-1725
Preprint. Discussion started: 6 September 2023

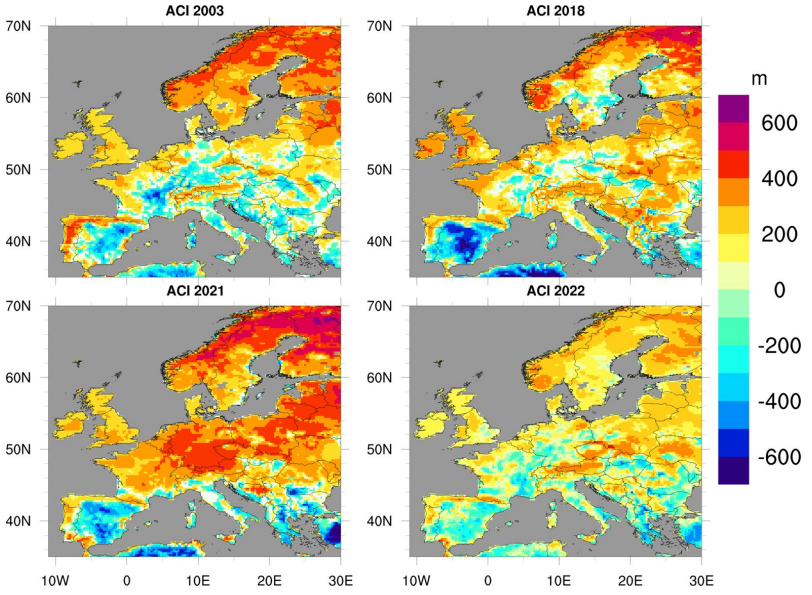

Figure 14. ACI LH-HLCL for the warmest and driest summer seasons 2003, 2018, and 2022 as well as for the very warm summer 2021.

310

4.2.2 Warm and wet summer seasons

Compared to the warm and dry summer seasons, 2002, 2007, and 2017 show the same coastal effect on the ACI LH-CAPE Fig. 15) as the warm and dry seasons, while coupling hot spots are seen over East and Southeast Europe. The latter appears to be a tail of the severe Russian heat wave (Becker et al., 2022). The LCL deficit south of 47°N
315 is often negative which is like during the warm and dry summers while the LCL deficit is always negative north of 50°N pointing to more favorable conditions for cloud and precipitation development. This is also reflected in positive soil moisture and precipitation anomalies (Fig. 7 and Fig. 8). The ACI LH-HLCL (Fig. 16) shows always positive values north of 44°N showing that LH influences the height of the lifted condensation level. Together with a negative LCL deficit this points to favorable conditions for the development of convection.

320

https://doi.org/10.5194/egusphere-2023-1725
Preprint. Discussion started: 6 September 2023

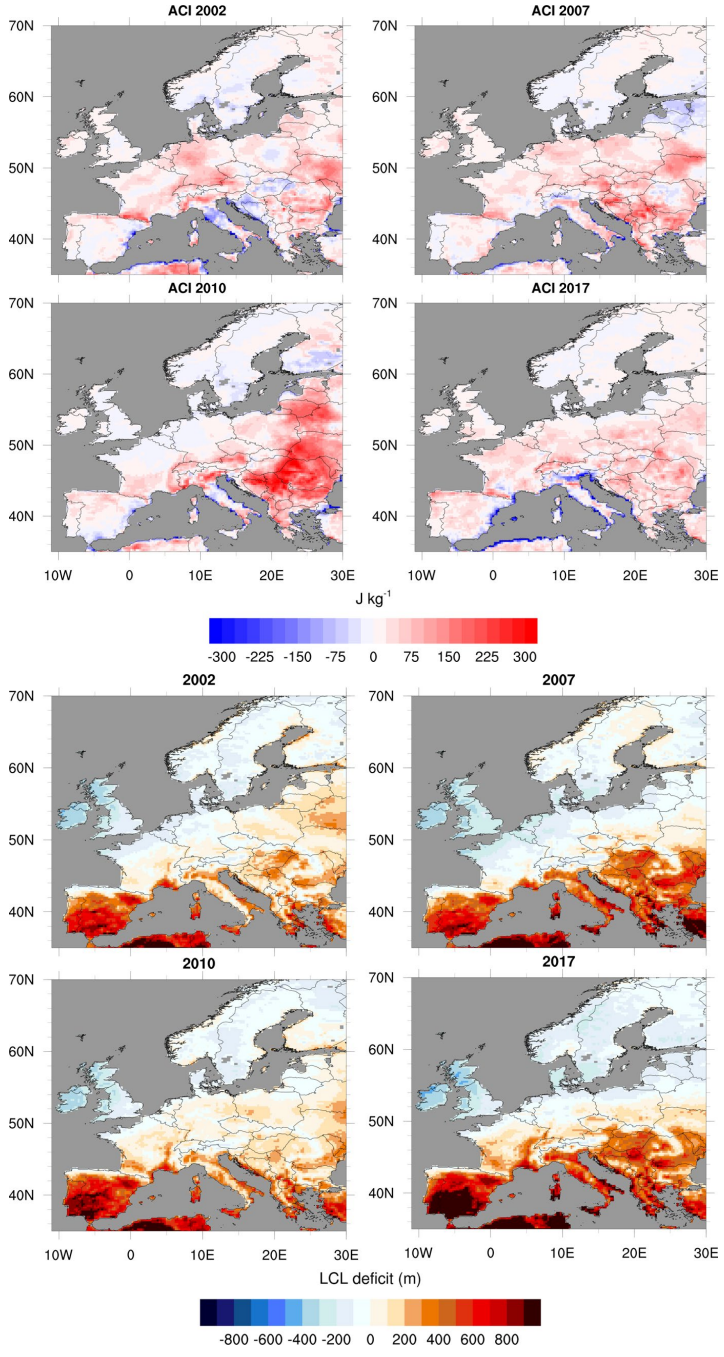

Figure 15. ACI LH-CAPE (1st and 2nd row) and LCL deficit (bottom rows) for the warm and wet summers 2002, 2007, 2010, and 2017.

https://doi.org/10.5194/egusphere-2023-1725
Preprint. Discussion started: 6 September 2023

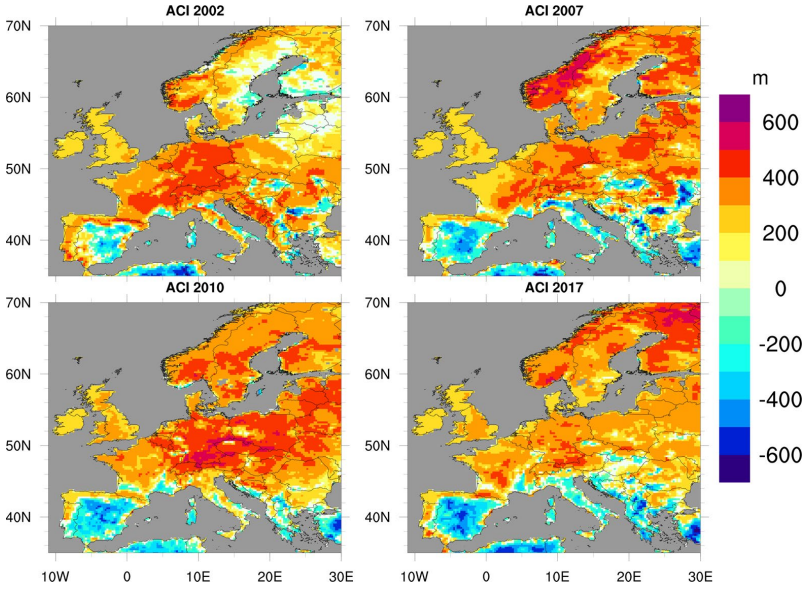

Figure 16. Same as Fig. 15 but for the warm and wet summer seasons 2002, 2007, 2010, and 2017.

6 Summary and Discussion

This paper describes the variability of the LA coupling strength of the warm summer seasons 1991-2022 which became the dominant situation over Europe since 2010. The summer seasons were classified according to 2-m temperature anomalies based on ERA5 (Hersbach et al., 2020) and precipitation anomalies based on E-OBS (Cornes et al., 2018) in the categories warm-dry and warm-wet. The reference period for the calculation of the anomalies was 1991-2020 (WMO, 2017). To further support our analysis, anomalies of the 500 hPa geopotential and volumetric root zone soil moisture, derived from ERA5, were considered in addition.

The analysis of the LA coupling strength was performed by means of different indices (Dirmeyer, 2011; Santanello et al., 2018) and by applying the coupling metrics framework provided by Tawfik (2015). All indices were calculated from ERA5 data using daytime values between 06 UTC and 18 UTC for each day (Yin et al., 2023).

According to Rousi et al. (2022) the frequency of the occurrence of heat waves is accelerating over Europe in the last 30-40 years where the large scale circulation pattern often features mid- and upper troposphere blocking situation leading to a split of the jet stream towards the Arctic and the Mediterranean. As the jet stream is an important feature for the European weather, it can also alter the near surface flow conditions in West and Central Europe (Laurila et al., 2021) while in other regions like the Mediterranean and East Europe, soil moisture preconditioning is more important as the impact of the jet stream becomes weaker (Prodhomme et al., 2022).

Our results revealed that warm and dry summer are usually characterized by positive geopotential anomalies throughout Europe (Kueh and Lin, 2020; Rousi et al., 2023) while the warm and wet summers show non-uniform anomaly pattern. The strong geopotential anomalies are linked to considerable positive 2-m temperature anomalies and the warm and dry summer seasons are usually characterized by a strong dry soil moisture anomaly.

During the warm and dry summer seasons, the TCI η-LH shows a strong coupling throughout major parts of Europe indicating that variations of η drive LH which was also observed in a study of Warrach-Sagi et al. (2022).

https://doi.org/10.5194/egusphere-2023-1725
Preprint. Discussion started: 6 September 2023

As the correlation SH-LH is mostly negative south of 45°N, together with the positive TCI this points to a strong limitation of evapotranspiration by insufficient root zone soil moisture and low LAI which is usually the case in South Europe (see Fig. S7c,d). At the same time, the correlation between SH and LH is usually positive north of 45°N. This points towards that evapotranspiration is limited by the incoming energy (Knist et al., 2017). Over Scandinavia, the TCI became less strong or even negative which, together with positive SH-LH correlations point towards sufficient root zone soil moisture availability for surface evapotranspiration.

The three most hot and dry summers of 2003, 2018, and 2022 show positive TCIs up to 60 °N without exception where a pronounced dry soil moisture anomaly is present. 2018 started with an already warmer than average and much drier spring season over Germany leading to a severe drought due to a severe soil moisture depletion (Rousi et al., 2023) and an exceptionally low LAI (Fig. S7c). Dirmeyer et al. (2021) found that when the volumetric soil moisture content falls below a critical value, surface heating becomes extremely more sensitive to further surface drying amplifying the intensity of heatwaves. Although it is categorized as warm wet in our study, summer 2021 illustrates an exception. A strong SW-NE temperature anomaly gradient associated with a strong positive 500 hPa geopotential anomaly north of 55°N was evident. A major event during this summer was the flood event mid of July 2021 which affected larger areas of West and Central Europe and lead to well extreme precipitation of more than 150 mm d^{-1} (Ludwig et al., 2023; Mohr et al., 2023). This heavy precipitation event was caused by a slow moving small-scale low-pressure system and led to longer lasting positive soil moisture anomaly. The anomaly is directly reflected in low TCI values and a strong correlation between LH and SH as enough surface moisture was available for evaporation.

During the four wet and warm summer seasons 2002, 2007, 2010, and 2017 the TCI η-LH is positive over Central Europe indicating a sufficient soil moisture availability for evapotranspiration confirmed by the positive correlation between LH and SH. A common feature of all evaluated summer seasons is the anticorrelation of LH and SH south of 44 °N. These regions are usually water-limited thus leading to limited evapotranspiration further reducing LH. As enough incoming energy is present, this further enhances SH and thus could further intensify drought periods in these regions.

During the warm and dry summer seasons, the ACI LH-CAPE shows coupling hot-spots over Southeast and East Europe as well as over the Baltic states. They were also observed in the study of Jach et al. (2022) who applied a climate temperature change signal to an existing 30 year simulation and evaluated the CTP-HI_{low} feedback metric (Findell and Eltahir, 2003b, 2003a). In contrast to the cold and wet years, the LCL deficit is mostly positive over Central and South Europe which is associated with a negative precipitation anomaly over the respective areas. On the other hand, the negative LCL deficit over the British Isles is directly connected with a positive precipitation anomaly (especially 2019 and 2020) indicating that LA feedback processes were driven by low pressure systems. For the four warm and wet summer seasons a clear connection between the 500 hPa geopotential anomalies and the positive precipitation anomalies can be established suggesting large-scale driven precipitation . The TCI η-LH shows neutral or no coupling over Central Europe indicating an energy limited evapotranspiration which is confirmed by the positive SH-LH correlations north of 44°N. The ACI also indicates a coupling hot spot region over East and Southeast Europe hence no considerable divergence between warm and wet and warm and dry summer seasons. The LCL deficit in general is lower than during the warm and dry summers which points towards favorable conditions for cloud and precipitation development. As sufficient root zone soil moisture is available for surface evaporation, this leads to a moistening of the PBL and thus lowers the LCL.

https://doi.org/10.5194/egusphere-2023-1725
Preprint. Discussion started: 6 September 2023

ERA5 clearly outperforms its predecessor ERA-Interim (Dee et al., 2011) and makes use of sophisticated atmospheric data assimilation including satellite derived soil moisture data (Albergel et al., 2012) to its land-surface model (LSM) HTESSEL (Balsamo et al., 2009). Currently, ERA5 applies a static LAI climatology (Fig. S7b) which was derived from the period 2000-2008 (Boussetta et al., 2013; ECMWF, 2016). However, under a changing climate the interannual variability of LAI is increasing as observed by satellites in the Copernicus Global Land Service (CGLS) project (Fuster et al., 2020) (Fig. S7c,d). Data such as these could help to further improve, e.g., the simulated evapotranspiration.

A study of Denissen et al. (2020) found that LSMs tend to overestimate the critical soil moisture and thus evaporation becomes soil moisture limited too early. A recent study of Warrach-Sagi et al. (2022) using the LSM NOAH-MP (Niu et al., 2011) showed that, even on a convection permitting (CP) horizontal resolution, LA feedback strength tends to be underestimated when using a LAI climatology in numerical weather prediction (NWP) models as compared to including the dynamic vegetation model GECROS (Yin and van Laar, 2005). This is in contrast to the results of Denissen et al. (2020) indicating the need for further enhancements of the applied LSMs (Hersbach and Bell, 2022; He et al., 2023).

Our results show that the hydro-climatological conditions during each summer drive considerable interannual variability in LA coupling over Central Europe. Hot and dry conditions shift the terrestrial coupling to the moisture-limited regime, push the sensitivity of the HLCL on low LH, and through this switch gears to strongly positive LCL deficits which decreases the likelihood for locally triggered deep convection in this region. The increasing frequency of warm and dry years toward the second half of the study period hints toward a trend of extended periods of moisture-limitations for evapotranspiration. This suggests a growing influence of soil moisture variability on the meteorological conditions which was not as pronounced in the first half of the study period experiencing cooler and moister conditions. Though it requires more research to deepen the understanding of how different characteristics of large-scale circulation patterns such as surface wind patterns, horizontal moisture transport or the location of the center of a high- or low-pressure system influence the coupling or how dynamic vegetation-climate feedbacks do, we consider this work a valuable contribution to understanding land surface influences on extreme events. While further research is necessary to enhance our understanding of the complex interplay between various characteristics of large-scale circulation patterns, (including surface wind patterns, horizontal moisture transport, or the positioning of high- or low-pressure systems,) and their impact on coupling as well as influences of dynamic vegetation-climate feedbacks, we view this endeavor as a significant step towards understanding the role of land surface influences in extreme events.

Acknowledgements

TS was funded by the German Ministry of Education and Research (BMBF) project ClimXtreme (subproject LAFEP, grant number 01LP1902D). Copernicus Climate Change Service (2018) data was downloaded from the Copernicus Climate Change Service (C3S) Climate Data Store https://cds.climate.copernicus.eu/cdsapp#!/dataset/reanalysis-era5-single-levels?tab=overview. The results contain modified Copernicus Climate Change Service information 2020. Neither the European Commission nor ECMWF is responsible for any use that may be made of the Copernicus information or data it contains.

https://doi.org/10.5194/egusphere-2023-1725
Preprint. Discussion started: 6 September 2023

Code availability

The code used in this study to calculate the coupling indices is obtained from https://github.com/abtawfik/coupling-metrics. The NCL software package can be downloaded from https://www.ncl.ucar.edu/current_release.shtml.

Data availability

E-OBS data were downloaded from https://surfobs.climate.copernicus.eu/dataaccess/access_E-OBS.php and the ERA5 data are available at https://cds.climate.copernicus.eu/cdsapp#!/dataset/reanalysis-era5-single-levels?tab=overview.

Author contributions

TS, LJ, VW, and KWS conceived the idea for the LA feedback study presented here. TS processed the data and graphics and performed the analyses together with LJ and KWS. The paper was written by TS with support of all coauthors.

Competing interests

The authors declare that they have no competing interests.

References

Albergel, C., Rosnay, P. de, Balsamo, G., Isaksen, L., and Muñoz-Sabater, J.: Soil Moisture Analyses at ECMWF: Evaluation Using Global Ground-Based In Situ Observations, Journal of Hydrometeorology, 13, 1442–1460, https://doi.org/10.1175/JHM-D-11-0107.1, 2012.

Balsamo, G., Beljaars, A., Scipal, K., Viterbo, P., van den Hurk, B., Hirschi, M., and Betts, A. K.: A Revised Hydrology for the ECMWF Model: Verification from Field Site to Terrestrial Water Storage and Impact in the Integrated Forecast System, Journal of Hydrometeorology, 10, 623–643, https://doi.org/10.1175/2008JHM1068.1, 2009.

Becker, F. N., Fink, A. H., Bissolli, P., and Pinto, J. G.: Towards a more comprehensive assessment of the intensity of historical European heat waves (1979–2019), Atmospheric Science Letters, 23, https://doi.org/10.1002/ASL.1120, 2022.

Boeing, F., Rakovec, O., Kumar, R., Samaniego, L., Schrön, M., Hildebrandt, A., Rebmann, C., Thober, S., Müller, S., Zacharias, S., Bogena, H., Schneider, K., Kiese, R., Attinger, S., and Marx, A.: High-resolution drought simulations and comparison to soil moisture observations in Germany, Hydrol. Earth Syst. Sci., 26, 5137–5161, https://doi.org/10.5194/hess-26-5137-2022, 2022.

Bolton, D.: The Computation of Equivalent Potential Temperature, Mon. Wea. Rev., 108, 1046–1053, https://doi.org/10.1175/1520-0493(1980)108<1046:TCOEPT>2.0.CO;2, 1980.

Boussetta, S., Balsamo, G., Beljaars, A., Kral, T., and Jarlan, L.: Impact of a satellite-derived leaf area index monthly climatology in a global numerical weather prediction model, International Journal of Remote Sensing, 34, 3520–3542, https://doi.org/10.1080/01431161.2012.716543, 2013.

https://doi.org/10.5194/egusphere-2023-1725
Preprint. Discussion started: 6 September 2023

Brown, D., Brownrigg, R., Haley, M., and Huang, W.: NCAR Command Language (NCL), UCAR/NCAR - Computational and Information Systems Laboratory (CISL), 2012.

C3S: Summer 2022 Europe's hottest on record: Press release, Copernicus Climate Change Service, https://climate.copernicus.eu/copernicus-summer-2022-europes-hottest-record, last access: 18 July 2023, 2022.

C3S: Precipitation, relative humidity and soil moisture for June 2021, Copernicus Climate Change Service, https://climate.copernicus.eu/precipitation-relative-humidity-and-soil-moisture-june-2021, last access: 30 October 2022, 2021a.

C3S: Precipitation, relative humidity and soil moisture for May 2021, Copernicus Climate Change Service, https://climate.copernicus.eu/precipitation-relative-humidity-and-soil-moisture-may-2021, last access: 30 October 2022, 2021b.

C3S: Dry and warm spring and summer, Copernicus Climate Change Service, https://climate.copernicus.eu/dry-and-warm-spring-and-summer, last access: 14 November 2022, 2018.

C3S: Climate in 2017 - Focus Region: Southwest Europe, Copernicus Climate Change Service, https://climate.copernicus.eu/climate-2017-focus-region-southwest-europe, last access: 24 February 2023, 2017.

Copernicus Climate Change Service: ERA5 hourly data on single levels from 1959 to present, 2018.

Cornes, R. C., van der Schrier, G., van den Besselaar, E. J. M., and Jones, P. D.: An Ensemble Version of the E-OBS Temperature and Precipitation Data Sets, J. Geophys. Res. Atmos., 123, 9391–9409, https://doi.org/10.1029/2017JD028200, available at: https://agupubs.onlinelibrary.wiley.com/doi/full/10.1029/2017JD028200, 2018.

Dee, D. P., Uppala, S. M., Simmons, A. J., Berrisford, P., Poli, P., Kobayashi, S., Andrae, U., Balmaseda, M. A., Balsamo, G., Bauer, P., Bechtold, P., Beljaars, A. C. M., van de Berg, L., Bidlot, J., Bormann, N., Delsol, C., Dragani, R., Fuentes, M., Geer, A. J., Haimberger, L., Healy, S. B., Hersbach, H., Hólm, E. V., Isaksen, L., Kållberg, P., Köhler, M., Matricardi, M., McNally, A. P., Monge-Sanz, B. M., Morcrette, J.-J., Park, B.-K., Peubey, C., Rosnay, P. de, Tavolato, C., Thépaut, J.-N., and Vitart, F.: The ERA-Interim reanalysis: configuration and performance of the data assimilation system, Q.J.R. Meteorol. Soc., 137, 553–597, https://doi.org/10.1002/qj.828, 2011.

Denissen, J. M. C., Teuling, A. J., Pitman, A. J., Koirala, S., Migliavacca, M., Li, W., Reichstein, M., Winkler, A. J., Zhan, C., and Orth, R.: Widespread shift from ecosystem energy to water limitation with climate change, Nat. Clim. Chang., 12, 677–684, https://doi.org/10.1038/s41558-022-01403-8, 2022.

Denissen, J. M., Teuling, A. J., Reichstein, M., and Orth, R.: Critical Soil Moisture Derived From Satellite Observations Over Europe, Journal of Geophysical Research: Atmospheres, 125, https://doi.org/10.1029/2019JD031672, 2020.

Di Capua, G., Sparrow, S., Kornhuber, K., Rousi, E., Osprey, S., Wallom, D., van den Hurk, B., and Coumou, D.: Drivers behind the summer 2010 wave train leading to Russian heatwave and Pakistan flooding, npj Clim Atmos Sci, 4, https://doi.org/10.1038/s41612-021-00211-9, 2021.

Dirmeyer, P. A.: The terrestrial segment of soil moisture-climate coupling, Geophys. Res. Lett., 38, n/a-n/a, https://doi.org/10.1029/2011GL048268, 2011.

https://doi.org/10.5194/egusphere-2023-1725
Preprint. Discussion started: 6 September 2023

Dirmeyer, P. A., Balsamo, G., Blyth, E. M., Morrison, R., and Cooper, H. M.: Land-Atmosphere Interactions Exacerbated the Drought and Heatwave Over Northern Europe During Summer 2018, AGU Advances, 2, https://doi.org/10.1029/2020AV000283, 2021.

Dirmeyer, P. A., Wang, Z., Mbuh, M. J., and Norton, H. E.: Intensified land surface control on boundary layer growth in a changing climate, Geophys. Res. Lett., 41, 1290–1294, https://doi.org/10.1002/2013GL058826, 2014.

Duan, S. Q., Findell, K. L., and Wright, J. S.: Three Regimes of Temperature Distribution Change Over Dry Land, Moist Land, and Oceanic Surfaces, Geophys. Res. Lett., 47, https://doi.org/10.1029/2020GL090997, 2020.

ECMWF: IFS Documentation CY41R2 - Part IV: Physical Processes, 2016.

Findell, K. L. and Eltahir, E. A. B.: Atmospheric Controls on Soil Moisture–Boundary Layer Interactions. Part I: Framework Development, Journal of Hydrometeorology, 4, 552–569, https://doi.org/10.1175/1525-7541(2003)004%3C0552:ACOSML%3E2.0.CO;2, 2003a.

Findell, K. L. and Eltahir, E. A. B.: Atmospheric Controls on Soil Moisture–Boundary Layer Interactions. Part II: Feedbacks within the Continental United States, Journal of Hydrometeorology, 4, 570–583, https://doi.org/10.1175/1525-7541(2003)004%3C0570:ACOSML%3E2.0.CO;2, 2003b.

Findell, K. L., Gentine, P., Lintner, B. R., and Guillod, B. P.: Data Length Requirements for Observational Estimates of Land–Atmosphere Coupling Strength, Journal of Hydrometeorology, 16, 1615–1635, https://doi.org/10.1175/JHM-D-14-0131.1, 2015.

Fuster, B., Sánchez-Zapero, J., Camacho, F., García-Santos, V., Verger, A., Lacaze, R., Weiss, M., Baret, F., and Smets, B.: Quality Assessment of PROBA-V LAI, fAPAR and fCOVER Collection 300 m Products of Copernicus Global Land Service, Remote Sensing, 12, 1017, https://doi.org/10.3390/rs12061017, 2020.

García-Herrera, R., Díaz, J., Trigo, R. M., Luterbacher, J., and Fischer, E. M.: A Review of the European Summer Heat Wave of 2003, Critical Reviews in Environmental Science and Technology, 40, 267–306, https://doi.org/10.1080/10643380802238137, 2010.

García-Monteiro, S., Sobrino, J. A., Julien, Y., Sòria, G., and Skokovic, D.: Surface Temperature trends in the Mediterranean Sea from MODIS data during years 2003–2019, Regional Studies in Marine Science, 49, 102086, https://doi.org/10.1016/j.rsma.2021.102086, 2022.

Georgakakos, K. P. and Bras, R. L.: A hydrologically useful station precipitation model: 1. Formulation, Water Resour. Res., 20, 1585–1596, https://doi.org/10.1029/WR020i011p01585, 1984.

Grams, C. M., Binder, H., Pfahl, S., Piaget, N., and Wernli, H.: Atmospheric processes triggering the central European floods in June 2013, Nat. Hazards Earth Syst. Sci., 14, 1691–1702, https://doi.org/10.5194/nhess-14-1691-2014, 2014.

Guo, Z. and Dirmeyer, P. A.: Interannual Variability of Land–Atmosphere Coupling Strength, Journal of Hydrometeorology, 14, 1636–1646, https://doi.org/10.1175/JHM-D-12-0171.1, 2013.

Guo, Z., Dirmeyer, P. A., Koster, R. D., Sud, Y. C., Bonan, G., Oleson, K. W., Chan, E., Verseghy, D., Cox, P., Gordon, C. T., McGregor, J. L., Kanae, S., Kowalczyk, E., Lawrence, D., Liu, P., Mocko, D., Lu, C.-H., Mitchell, K., Malyshev, S., McAvaney, B., Oki, T., Yamada, T., Pitman, A., Taylor, C. M., Vasic, R., and Xue, Y.: GLACE: The Global Land–Atmosphere Coupling Experiment. Part II: Analysis, Journal of Hydrometeorology, 7, 611–625, https://doi.org/10.1175/JHM511.1, 2006.

https://doi.org/10.5194/egusphere-2023-1725
Preprint. Discussion started: 6 September 2023

Hauser, M., Orth, R., and Seneviratne, S. I.: Role of soil moisture versus recent climate change for the 2010 heat wave in western Russia, Geophys. Res. Lett., 43, 2819–2826, https://doi.org/10.1002/2016GL068036, 2016.

He, C., Valayamkunnath, P., Barlage, M., Chen, F., Gochis, D., Cabell, R., Schneider, T., Rasmussen, R., Niu, G.-Y., Yang, Z.-L., Niyogi, D., and Ek, M.: Modernizing the open-source community Noah-MP land surface model (version 5.0) with enhanced modularity, interoperability, and applicability, 2023.

Hersbach, H. and Bell, B.: Characteristics of ERA5 and innovations for ERA6, 5th C3S General Assembly, https://climate.copernicus.eu/sites/default/files/2022-09/S3_Hans_Hersbach_v1.pdf, last access: 4 July 2023, 2022.

Hersbach, H., Bell, B., Berrisford, P., Hirahara, S., Horányi, A., Muñoz-Sabater, J., Nicolas, J., Peubey, C., Radu, R., Schepers, D., Simmons, A., Soci, C., Abdalla, S., Abellan, X., Balsamo, G., Bechtold, P., Biavati, G., Bidlot, J., Bonavita, M., Chiara, G., Dahlgren, P., Dee, D., Diamantakis, M., Dragani, R., Flemming, J., Forbes, R., Fuentes, M., Geer, A., Haimberger, L., Healy, S., Hogan, R. J., Hólm, E., Janisková, M., Keeley, S., Laloyaux, P., Lopez, P., Lupu, C., Radnoti, G., Rosnay, P., Rozum, I., Vamborg, F., Villaume, S., and Thépaut, J.-N.: The ERA5 global reanalysis, Q.J.R. Meteorol. Soc., 146, 1999–2049, https://doi.org/10.1002/qj.3803, 2020.

Huebener, H., Hoffmann, P., Keuler, K., Pfeifer, S., Ramthun, H., Spekat, A., Steger, C., and Warrach-Sagi, K.: Deriving user-informed climate information from climate model ensemble results, Adv. Sci. Res., 14, 261–269, https://doi.org/10.5194/asr-14-261-2017, 2017.

Jach, L., Schwitalla, T., Branch, O., Warrach-Sagi, K., and Wulfmeyer, V.: Sensitivity of land–atmosphere coupling strength to changing atmospheric temperature and moisture over Europe, Earth Syst. Dynam., 13, 109–132, https://doi.org/10.5194/esd-13-109-2022, 2022.

Jach, L., Warrach-Sagi, K., Ingwersen, J., Kaas, E., and Wulfmeyer, V.: Land Cover Impacts on Land-Atmosphere Coupling Strength in Climate Simulations With WRF Over Europe, Journal of Geophysical Research: Atmospheres, 125, https://doi.org/10.1029/2019JD031989, 2020.

Knist, S., Goergen, K., Buonomo, E., Christensen, O. B., Colette, A., Cardoso, R. M., Fealy, R., Fernández, J., García-Díez, M., Jacob, D., Kartsios, S., Katragkou, E., Keuler, K., Mayer, S., van Meijgaard, E., Nikulin, G., Soares, P. M. M., Sobolowski, S., Szepszo, G., Teichmann, C., Vautard, R., Warrach-Sagi, K., Wulfmeyer, V., and Simmer, C.: Land-atmosphere coupling in EURO-CORDEX evaluation experiments, J. Geophys. Res. Atmos., 122, 79–103, https://doi.org/10.1002/2016JD025476, 2017.

Kornhuber, K., Petoukhov, V., Petri, S., Rahmstorf, S., and Coumou, D.: Evidence for wave resonance as a key mechanism for generating high-amplitude quasi-stationary waves in boreal summer, Clim Dyn, 49, 1961–1979, https://doi.org/10.1007/s00382-016-3399-6, 2017.

Koster, R. D., Dirmeyer, P. A., Guo, Z., Bonan, G., Chan, E., Cox, P., Gordon, C. T., Kanae, S., Kowalczyk, E., Lawrence, D., Liu, P., Lu, C.-H., Malyshev, S., McAvaney, B., Mitchell, K., Mocko, D., Oki, T., Oleson, K., Pitman, A., Sud, Y. C., Taylor, C. M., Verseghy, D., Vasic, R., Xue, Y., and Yamada, T.: Regions of strong coupling between soil moisture and precipitation, Science (New York, N.Y.), 305, 1138–1140, https://doi.org/10.1126/science.1100217, 2004.

Kueh, M.-T. and Lin, C.-Y.: The 2018 summer heatwaves over northwestern Europe and its extended-range prediction, Scientific reports, 10, 19283, https://doi.org/10.1038/s41598-020-76181-4, 2020.

https://doi.org/10.5194/egusphere-2023-1725
Preprint. Discussion started: 6 September 2023

Laurila, T. K., Sinclair, V. A., and Gregow, H.: Climatology, variability, and trends in near-surface wind speeds over the North Atlantic and Europe during 1979–2018 based on ERA5, Int J Climatol, 41, 2253–2278, https://doi.org/10.1002/joc.6957, 2021.

Lhotka, O. and Kyselý, J.: The 2021 European Heat Wave in the Context of Past Major Heat Waves, Earth and Space Science, 9, https://doi.org/10.1029/2022EA002567, 2022.

Lo, M.-H., Wu, W.-Y., Tang, L. I., Ryu, D., Rashid, M., and Wu, R.-J.: Temporal Changes in Land Surface Coupling Strength: An Example in a Semi-Arid Region of Australia, Journal of Climate, 34, 1503–1513, https://doi.org/10.1175/JCLI-D-20-0250.1, 2021.

Ludwig, P., Ehmele, F., Franca, M. J., Mohr, S., Caldas-Alvarez, A., Daniell, J. E., Ehret, U., Feldmann, H., Hundhausen, M., Knippertz, P., Küpfer, K., Kunz, M., Mühr, B., Pinto, J. G., Quinting, J., Schäfer, A. M., Seidel, F., and Wisotzky, C.: A multi-disciplinary analysis of the exceptional flood event of July 2021 in central Europe – Part 2: Historical context and relation to climate change, Nat. Hazards Earth Syst. Sci., 23, 1287–1311, https://doi.org/10.5194/nhess-23-1287-2023, 2023.

Miralles, D. G., Gentine, P., Seneviratne, S. I., and Teuling, A. J.: Land-atmospheric feedbacks during droughts and heatwaves: state of the science and current challenges, Annals of the New York Academy of Sciences, 1436, 19–35, https://doi.org/10.1111/nyas.13912, 2019.

Miralles, D. G., Teuling, A. J., van Heerwaarden, C. C., and Vilà-Guerau de Arellano, J.: Mega-heatwave temperatures due to combined soil desiccation and atmospheric heat accumulation, Nat. Geosci., 7, 345–349, https://doi.org/10.1038/ngeo2141, 2014.

Mohr, S., Ehret, U., Kunz, M., Ludwig, P., Caldas-Alvarez, A., Daniell, J. E., Ehmele, F., Feldmann, H., Franca, M. J., Gattke, C., Hundhausen, M., Knippertz, P., Küpfer, K., Mühr, B., Pinto, J. G., Quinting, J., Schäfer, A. M., Scheibel, M., Seidel, F., and Wisotzky, C.: A multi-disciplinary analysis of the exceptional flood event of July 2021 in central Europe – Part 1: Event description and analysis, Nat. Hazards Earth Syst. Sci., 23, 525–551, https://doi.org/10.5194/nhess-23-525-2023, 2023.

Müller, O. V., Vidale, P. L., Vannière, B., Schiemann, R., Senan, R., Haarsma, R. J., and Jungclaus, J. H.: Land–Atmosphere Coupling Sensitivity to GCMs Resolution: A Multimodel Assessment of Local and Remote Processes in the Sahel Hot Spot, Journal of Climate, 34, 967–985, https://doi.org/10.1175/JCLI-D-20-0303.1, 2021.

Niu, G.-Y., Yang, Z.-L., Mitchell, K. E., Chen, F., Ek, M. B., Barlage, M., Kumar, A., Manning, K., Niyogi, D., Rosero, E., Tewari, M., and Xia, Y.: The community Noah land surface model with multiparameterization options (Noah-MP): 1. Model description and evaluation with local-scale measurements, J. Geophys. Res., 116, https://doi.org/10.1029/2010JD015139, 2011.

Orth, R.: When the Land Surface Shifts Gears, AGU Advances, 2, https://doi.org/10.1029/2021AV000414, 2021.

Ossó, A., Allan, R. P., Hawkins, E., Shaffrey, L., and Maraun, D.: Emerging new climate extremes over Europe, Clim Dyn, 58, 487–501, https://doi.org/10.1007/s00382-021-05917-3, 2022.

Piper, D., Kunz, M., Ehmele, F., Mohr, S., Mühr, B., Kron, A., and Daniell, J.: Exceptional sequence of severe thunderstorms and related flash floods in May and June 2016 in Germany – Part 1: Meteorological background, Nat. Hazards Earth Syst. Sci., 16, 2835–2850, https://doi.org/10.5194/nhess-16-2835-2016, 2016.

https://doi.org/10.5194/egusphere-2023-1725
Preprint. Discussion started: 6 September 2023

Prodhomme, C., Materia, S., Ardilouze, C., White, R. H., Batté, L., Guemas, V., Fragkoulidis, G., and García-Serrano, J.: Seasonal prediction of European summer heatwaves, Clim Dyn, 58, 2149–2166, https://doi.org/10.1007/s00382-021-05828-3, 2022.

Rakovec, O., Samaniego, L., Hari, V., Markonis, Y., Moravec, V., Thober, S., Hanel, M., and Kumar, R.: The 2018–2020 Multi-Year Drought Sets a New Benchmark in Europe, Earth's Future, 10, https://doi.org/10.1029/2021EF002394, 2022.

Rousi, E., Fink, A. H., Andersen, L. S., Becker, F. N., Beobide-Arsuaga, G., Breil, M., Cozzi, G., Heinke, J., Jach, L., Niermann, D., Petrovic, D., Richling, A., Riebold, J., Steidl, S., Suarez-Gutierrez, L., Tradowsky, J. S., Coumou, D., Düsterhus, A., Ellsäßer, F., Fragkoulidis, G., Gliksman, D., Handorf, D., Haustein, K., Kornhuber, K., Kunstmann, H., Pinto, J. G., Warrach-Sagi, K., and Xoplaki, E.: The extremely hot and dry 2018 summer in central and northern Europe from a multi-faceted weather and climate perspective, Nat. Hazards Earth Syst. Sci., 23, 1699–1718, https://doi.org/10.5194/nhess-23-1699-2023, 2023.

Rousi, E., Kornhuber, K., Beobide-Arsuaga, G., Luo, F., and Coumou, D.: Accelerated western European heatwave trends linked to more-persistent double jets over Eurasia, Nature communications, 13, 3851, https://doi.org/10.1038/s41467-022-31432-y, 2022.

Santanello, J. A., Dirmeyer, P. A., Ferguson, C. R., Findell, K. L., Tawfik, A. B., Berg, A., Ek, M., Gentine, P., Guillod, B. P., van Heerwaarden, C., Roundy, J., and Wulfmeyer, V.: Land–Atmosphere Interactions: The LoCo Perspective, Bulletin of the American Meteorological Society, 99, 1253–1272, https://doi.org/10.1175/BAMS-D-17-0001.1, 2018.

Santanello, J. A., Peters-Lidard, C. D., and Kumar, S. V.: Diagnosing the Sensitivity of Local Land–Atmosphere Coupling via the Soil Moisture–Boundary Layer Interaction, Journal of Hydrometeorology, 12, 766–786, https://doi.org/10.1175/JHM-D-10-05014.1, 2011.

Santanello, J. A., Peters-Lidard, C. D., Kumar, S. V., Alonge, C., and Tao, W.-K.: A Modeling and Observational Framework for Diagnosing Local Land–Atmosphere Coupling on Diurnal Time Scales, Journal of Hydrometeorology, 10, 577–599, https://doi.org/10.1175/2009JHM1066.1, 2009.

Schulzweida, U.: CDO User Guide, 2022.

Schumacher, D. L., Keune, J., Dirmeyer, P., and Miralles, D. G.: Drought self-propagation in drylands due to land-atmosphere feedbacks, Nat. Geosci., 15, 262–268, https://doi.org/10.1038/s41561-022-00912-7, 2022.

Seneviratne, S. I., Corti, T., Davin, E. L., Hirschi, M., Jaeger, E. B., Lehner, I., Orlowsky, B., and Teuling, A. J.: Investigating soil moisture–climate interactions in a changing climate: A review, Earth-Science Reviews, 99, 125–161, https://doi.org/10.1016/j.earscirev.2010.02.004, 2010.

Seneviratne, S. I., Lüthi, D., Litschi, M., and Schär, C.: Land-atmosphere coupling and climate change in Europe, Nature, 443, 205–209, https://doi.org/10.1038/nature05095, 2006.

Spensberger, C., Madonna, E., Boettcher, M., Grams, C. M., Papritz, L., Quinting, J. F., Röthlisberger, M., Sprenger, M., and Zschenderlein, P.: Dynamics of concurrent and sequential Central European and Scandinavian heatwaves, Q.J.R. Meteorol. Soc., 146, 2998–3013, https://doi.org/10.1002/qj.3822, 2020.

Stephens, G., Polcher, J., Zeng, X., van Oevelen, P., Poveda, G., Bosilovich, M., Ahn, M.-H., Balsamo, G., Duan, Q., Hegerl, G., Jakob, C., Lamptey, B., Leung, R., Piles, M., Su, Z., Dirmeyer, P., Findell, K. L., Verhoef, A., Ek, M., L'Ecuyer, T., Roca, R., Nazemi, A., Dominguez, F., Klocke, D., and Bony, S.: The First 30 Years of GEWEX, Bulletin of the American Meteorological Society, 104, E126-E157, https://doi.org/10.1175/BAMS-D-22-0061.1, 2023.

https://doi.org/10.5194/egusphere-2023-1725
Preprint. Discussion started: 6 September 2023

Tawfik, A. B.: Terrestrial coupling indices, https://github.com/abtawfik/coupling-metrics/tree/master/terrestrial_coupling_index, last access: 2 November 2022, 2015.

Toreti, A., Bavera, D., Acosta Navarro, J., Cammalleri, C., Jager, A. de, Di Ciollo, C., Hrast Essenfelder, A., Maetens, W., Magni, D., Masante, D., Mazzeschi, M., Niemeyer, S., and Spinoni, J.: Drought in Europe August 2022, 2022.

Ukkola, A. M., Pitman, A. J., Donat, M. G., Kauwe, M. G. de, and Angélil, O.: Evaluating the Contribution of Land-Atmosphere Coupling to Heat Extremes in CMIP5 Models, Geophys. Res. Lett., 45, 9003–9012, https://doi.org/10.1029/2018GL079102, 2018.

van der Wiel, K., Batelaan, T. J., and Wanders, N.: Large increases of multi-year droughts in north-western Europe in a warmer climate, Clim Dyn, https://doi.org/10.1007/s00382-022-06373-3, 2022.

van Heerwaarden, C. C. and Teuling, A. J.: Disentangling the response of forest and grassland energy exchange to heatwaves under idealized land–atmosphere coupling, Biogeosciences, 11, 6159–6171, https://doi.org/10.5194/bg-11-6159-2014, 2014.

Warrach-Sagi, K., Ingwersen, J., Schwitalla, T., Troost, C., Aurbacher, J., Jach, L., Berger, T., Streck, T., and Wulfmeyer, V.: Noah-MP With the Generic Crop Growth Model Gecros in the WRF Model: Effects of Dynamic Crop Growth on Land-Atmosphere Interaction, Journal of Geophysical Research: Atmospheres, 127, https://doi.org/10.1029/2022JD036518, 2022.

Wehrli, K., Guillod, B. P., Hauser, M., Leclair, M., and Seneviratne, S. I.: Identifying Key Driving Processes of Major Recent Heat Waves, Journal of Geophysical Research: Atmospheres, 124, 11746–11765, https://doi.org/10.1029/2019JD030635, 2019.

Wei, J., Zhao, J., Chen, H., and Liang, X.-Z.: Coupling Between Land Surface Fluxes and Lifting Condensation Level: Mechanisms and Sensitivity to Model Physics Parameterizations, Journal of Geophysical Research: Atmospheres, 126, https://doi.org/10.1029/2020JD034313, 2021.

Werner, P. and Gerstengarbe, F.-W.: Catalog of the general weather situations of Europe, Potsdam Institute for Climate Impact Research, 2010.

WMO: Europe has hottest summer on record: EU Copernicus, World Meteorological Organization, https://public.wmo.int/en/media/news/europe-has-hottest-summer-record-eu-copernicus, last access: 14 November 2022, 2022a.

WMO: Precipitation, relative humidity and soil moisture for July 2022, World Meteorological Organization, https://climate.copernicus.eu/precipitation-relative-humidity-and-soil-moisture-july-2022, last access: 21 February 2023, 2022b.

WMO: Precipitation, relative humidity and soil moisture for July 2018, World Meteorological Organization, https://climate.copernicus.eu/precipitation-relative-humidity-and-soil-moisture-july-2018, last access: 21 February 2023, 2018.

WMO: WMO Guidelines on the Calculation of Climate Normals: Tech. Rep. WMO-No. 1203, World Meteorological Organization, 2017.

WMO: 2015 second hottest year on record for Europe, World Meteorological Organization, https://public.wmo.int/en/media/news/2015-second-hottest-year-record-europe, last access: 27 October 2022, 2015.

WMO: WMO STATEMENT ON THE STATUS OF THE GLOBAL CLIMATE IN 2003: Tech. Rep. WMO-No. 966, World Meteorological Organization, 2004.

https://doi.org/10.5194/egusphere-2023-1725
Preprint. Discussion started: 6 September 2023

Yin, X. and van Laar, H. H.: Crop systems dynamics, https://models.pps.wur.nl/gecros-detailed-eco-physiological-crop-growth-simulation-model-analyse-genotype-environment, last access: 1 March 2023, 2005.

Yin, Z., Findell, K. L., Dirmeyer, P., Shevliakova, E., Malyshev, S., Ghannam, K., Raoult, N., and Tan, Z.: Daytime-only mean data enhance understanding of land–atmosphere coupling, Hydrol. Earth Syst. Sci., 27, 861–872, https://doi.org/10.5194/hess-27-861-2023, 2023.

Zink, M., Samaniego, L., Kumar, R., Thober, S., Mai, J., Schäfer, D., and Marx, A.: The German drought monitor, Environ. Res. Lett., 11, 74002, https://doi.org/10.1088/1748-9326/11/7/074002, 2016.